AFRL-RH-FS-TR-2021-0009

Review of Skin and Cornea Laser-Induced Damage Thresholds from 1400 nm to 2000 nm and Broad-Spectrum Supra-Threshold Effects

Michael P. DeLisi
Xomalin G. Peralta
Brian J. Lund
Wallace E. Mitchell
SAIC

Chad A. Oian
Aaron F. Hoffman
711th Human Performance Wing
Airman Systems Directorate
Bioeffects Division
Optical Radiation Bioeffects Branch

30 June 2021
Interim Report for May 2021 to June 2021

Air Force Research Laboratory
711th Human Performance Wing
Airman Systems Directorate
Bioeffects Division
Optical Radiation Bioeffects Branch
JBSA Fort Sam Houston, Texas 78234

NOTICE AND SIGNATURE PAGE

Using Government drawings, specifications, or other data included in this document for any purpose other than Government procurement does not in any way obligate the U.S. Government. The fact that the Government formulated or supplied the drawings, specifications, or other data does not license the holder or any other person or corporation; or convey any rights or permission to manufacture, use, or sell any patented invention that may relate to them.

This report was cleared for public release by the 88th ABW Public Affairs Office and is available to the general public, including foreign nationals. Copies may be obtained from the Defense Technical Information Center (DTIC) (http://www.dtic.mil).

"Review of Skin and Cornea Laser-Induced Damage Thresholds from 1400 nm to 2000 nm and Broad-Spectrum Supra-Threshold Effects"

(AFRL-RH-FS-TR- 2021 - 0009) has been reviewed and is approved for publication in accordance with assigned distribution statement.

ROCKWELL.BENJAMIN.A.1231305358 Digitally signed by ROCKWELL.BENJAMIN.A.1231305358 Date: 2021.08.10 14:45:26 -05'00'

BENJAMIN A. ROCKWELL
Chief, Optical Radiation Bioeffects Branch

MILLER.STEPHANIE.A.1230536283 Digitally signed by MILLER.STEPHANIE.A.1230536283 Date: 2021.10.21 09:43:16 -05'00'

STEPHANIE A. MILLER, DR-IV, DAF
Chief, Bioeffects Division
Airman Systems Directorate
711th Human Performance Wing
Air Force Research Laboratory

This report is published in the interest of scientific and technical information exchange, and its publication does not constitute an official position of the U.S. Government.

REPORT DOCUMENTATION PAGE

Form Approved
OMB No. 0704-0188

1. REPORT DATE *(DD-MM-YYYY)*	**2. REPORT TYPE**	**3. DATES COVERED** *(From - To)*
30-06-2021	Interim Technical Report	May 2021 to June 2021

4. TITLE AND SUBTITLE
Review of Skin and Cornea Laser-Induced Damage Thresholds from 1400 nm to 2000 nm and Broad-Spectrum Supra-Threshold Effects

5a. CONTRACT NUMBER
FA8650-19-C-6024

5b. GRANT NUMBER

5c. PROGRAM ELEMENT NUMBER

6. AUTHOR(S)
Michael P. DeLisi, Xomalin G. Peralta, Brian J. Lund, Wallace E. Mitchell, Chad A. Oian, Aaron F. Hoffman

5d. PROJECT NUMBER

5e. TASK NUMBER

5f. WORK UNIT NUMBER
H10H

7. PERFORMING ORGANIZATION NAME(S) AND ADDRESS(ES)
Air Force Research Laboratory
711th Human Performance Wing
Airman Systems Directorate
Bioeffects Division
Optical Radiation Branch
JBSA, Fort Sam Houston, Texas 78234

SAIC
4141 Petroleum Rd
Fort Sam Houston, Texas 78234

8. PERFORMING ORGANIZATION REPORT

9. SPONSORING / MONITORING AGENCY NAME(S) AND ADDRESS(ES)
711th Human Performance Wing
Airman Systems Directorate
Bioeffects Division
Optical Radiation Branch
JBSA, Fort Sam Houston, Texas 78234

10. SPONSOR/MONITOR'S ACRONYM(S)
711 HPW/RHDO

11. SPONSOR/MONITOR'S REPORT NUMBER(S)
AFRL-RH-FS-TR-2021-0009

12. DISTRIBUTION / AVAILABILITY STATEMENT
Distribution Statement A. Approved for public release; distribution is unlimited. PA Case #: 502ABW-2021-0064. Approved: 10-29-2021. The opinions expressed on this document, electronic or otherwise, are solely those of the author(s). They do not represent an endorsement by or the views of the United States Air Force, the Department of Defense, or the United States Government.

13. SUPPLEMENTARY NOTES

14. ABSTRACT
Previous incarnations of dose response modeling have incorporated threshold-level damage endpoints at common laser wavelengths, but there is an increasing need to incorporate the full range of effects, those categorized as supra-threshold, over a broader wavelength region. This report reviews the published literature on threshold-level laser-induced damage to skin and cornea to highly-absorbed wavelengths, particularly in the region from 1400 to 2000 nm. Furthermore, it examines existing studies on laser-induced supra-threshold effects in skin and cornea across a broader wavelength region. A result of this review is recognition of the paucity of supra-threshold studies of laser skin interaction, particularly in terms of dose correlations to skin burn degrees and ablation thresholds. While several corneal ablation threshold studies exist, there is not a consensus in the literature on how to approach supra-threshold corneal damage in the injury region between the minimum visible lesion and ablation onset. We propose a sub-ablative "first degree" supra-threshold lesion metric, while designating the ablation onset as "second degree" supra-threshold.

15. SUBJECT TERMS

16. SECURITY CLASSIFICATION OF:			**17. LIMITATION OF ABSTRACT**	**18. NUMBER OF PAGES**	**19a. NAME OF RESPONSIBLE PERSON**
Unclassified					Chad A. Oian
a. REPORT	**b. ABSTRACT**	**c. THIS PAGE**	U	43	**19b. TELEPHONE NUMBER** *(include area code)*
U	U	U			NA

Standard Form 298 (Rev. 8-98)
Prescribed by ANSI Std. 239.18

This Page Intentionally Left Blank

TABLE OF CONTENTS

List of Figures

Page

1.0 SUMMARY

The continual development of high-energy lasers for military applications requires a robust and versatile approach to hazard analysis. Previous incarnations of dose response modeling incorporated threshold-level damage endpoints at common laser wavelengths, but there is an increasing need and desire to incorporate the full range of potential outcomes, those categorized as supra-threshold, over a broader wavelength region. This report reviews the published literature on threshold-level laser-induced damage to skin and cornea to highly-absorbed wavelengths, particularly in the region from 1400 nm to 2000 nm. Furthermore, it examines existing studies on laser-induced supra-threshold effects in skin and cornea across a broader wavelength region, given the limitations of the available studies. We tabulated the available skin and cornea damage and ablation thresholds for the reader's convenience. A result of this review is recognition of the paucity of supra-threshold studies of laser skin interactions, particularly in terms of dose correlations to skin burn degrees and ablation thresholds. While several corneal ablation threshold studies exist, there is not a consensus in the literature on how to approach supra-threshold corneal damage in the injury region between the minimum visible lesion and ablation onset. We propose a sub-ablative "first degree" supra-threshold lesion metric, while designating the ablation onset as "second degree" supra-threshold.

2.0 INTRODUCTION

The increased use of high-energy lasers in diverse areas and applications has repercussions on the approach to hazard analysis. While safety without the possibility of injury is the appropriate criteria for a highly-regulated environment, such as a laboratory or enclosed product, a risk-based approach is more feasible and useful in generalized or unknown settings. In the case of laser hazard analysis, risk is the combination of the probability of exposure and the severity of an injury resulting from that exposure. The severity of outcome is quantified by a dose response model relating level of exposure to probability and severity of effect. The research group at the 711th HPW/RHDO has been invested in the development of a laser exposure dose response model for over 15 years, and has incorporated hazard analyses relevant to both ocular and skin tissue [1-4]. Further details on the dose response model are available in several reports.

Up to this point, the hazard analysis included in the dose response model utilized data from threshold or onset-of-injury levels of laser-tissue damage. These data are typically gathered from *in vivo* studies using an appropriate animal subject and expressed in terms of minimum visible lesion (MVL) thresholds determined 24 hours after laser exposure for skin and 1 hour after laser exposure for cornea. However, as laser systems continue to increase in power and beam quality, it has become more relevant to consider higher levels of possible damage (supra-threshold damage) for hazard and risk assessment.

A substantial portion of the available experimental laser bioeffects research has focused on lasers operating in the ultraviolet (~100-400 nm), visible (~400-750 nm) and near-infrared or IR-A (~750-1400 nm) ranges. However, several recently developed and upcoming laser systems, such

as illuminator and designator lasers, have featured emission wavelengths between 1400 nm and 2000 nm. Various naming conventions would place these wavelengths in the short-wavelength infrared or IR-B range. These wavelengths feature much higher absorption in water than those in the visible and IR-A ranges. Biological tissues often contain large proportions of water, thus making them susceptible to laser-induced damage at such wavelengths, particularly at the surface where most of the laser energy is absorbed.

This document is intended to provide an overview of existing research into skin and ocular laser injury between 1400 nm and 2000 nm, as well as supra-threshold laser exposure in general. The goal of this overview is to assist in framing upcoming experiments intended to populate the dose response model with supra-threshold endpoints.

3.0 SKIN

Skin is an organ that covers the external surface of the body, functioning to protect other organs, regulate body temperature, and enable sensation and tactile response. The skin is multi-layered, composed broadly of the epidermis and dermis, each with its own distinct layers. The subcutaneous tissue, specifically connective tissue and fat, is not technically skin, but is often grouped with it for categorization purposes. Figure 1 demonstrates the layers of the skin and highlights various components and features of interest.

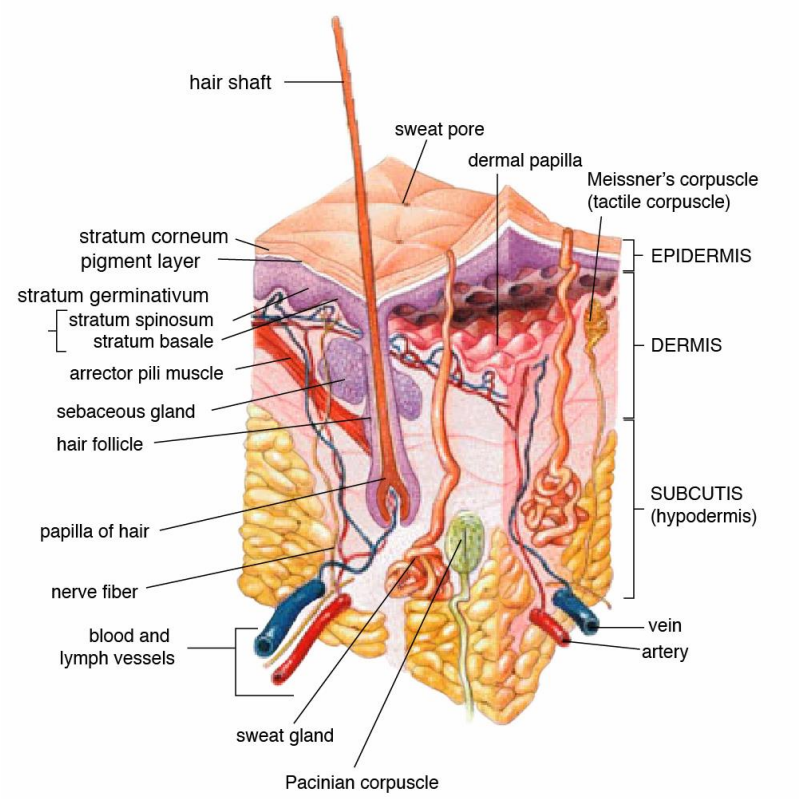

Figure 1. Skin anatomy (https://en.wikipedia.org/wiki/Dermis)

The epidermis is the outermost layer, and contains four or five layers, depending on the location on the body: the cornified layer (stratum corneum), the clear or translucent layer found only in the palms and soles (stratum lucidum), the granular layer (stratum granulosum), the spinous layer (stratum spinosum), and the basal or germinal layer (stratum basale or germinativum). These layers are shown in Figure 2. The epidermis is fairly thin, around ~100 µm but variable depending on body location, and regenerates quickly when damaged.

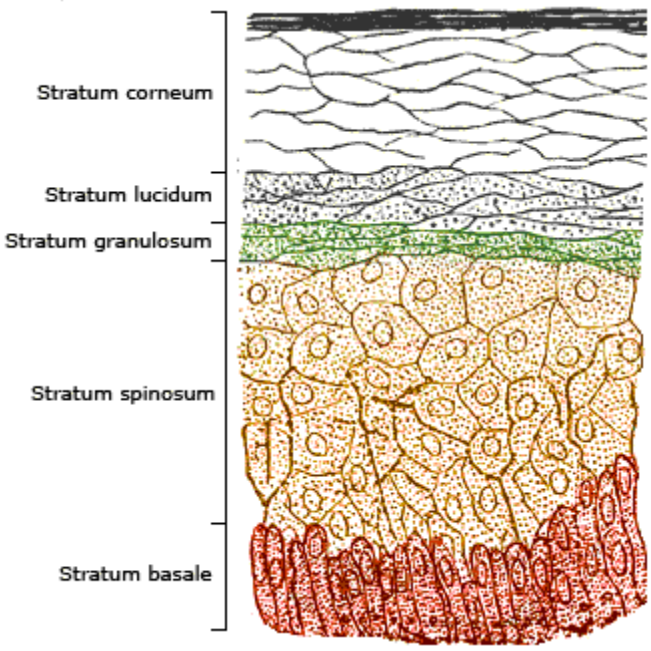

Figure 2. Layers of the epidermis (https://en.wikipedia.org/wiki/Epidermis)

The stratum corneum is composed primarily of dead cells that fulfill most of the barrier functions of the epidermis. The remaining layers are often referred to as the viable epidermis. The epidermis contains melanin, the primary component of pigmentation. Melanocyte cells located in the stratum basale synthesize melanin, which is then contained in organelles called melanosomes. Melanin is a highly-relevant chromophore when considering laser-skin interaction, as its absorption and scattering characteristics at given wavelengths are quite different than those of other chromophores such as water, hemoglobin, etc. This can result in protection of the dermis if the melanin absorption of light is high. However, in the wavelength region between 1400 nm and 2000 nm, the absorption of water is significantly higher than that of melanin and will dominate the resultant thermal loading of the skin tissues.

The dermis is substantially thicker than the epidermis (up to several millimeters, depending on body region) and contains many structures relevant to skin function, such as hair follicles, sweat glands, nerve endings, and vasculature. It is typically separated into the upper papillary dermis, which connects to the epidermis and contains more loosely arranged collagen fibers, and the lower reticular dermis, which is densely packed with collagen and contains most of the aforementioned structures.

In the context of laser-skin exposure, threshold-level damage is often fairly superficial and confined to the epidermis or possibly the upper portions of the papillary dermis. However, as dose increases and thermal energy propagates deeper, more portions of the dermis, and thus skin function, are impaired. Removal of the skin layers entirely through an ablation mechanism would severely compromise the underlying tissues and signify a substantial vector for infection.

3.1 Skin Laser Damage Thresholds From 1400 nm To 2000 nm

Several studies have investigated the minimum visible lesion laser damage thresholds to skin in the wavelength region between 1400 nm and 2000 nm, though most have been focused on the erbium glass laser range at 1540 nm and the thulium fiber laser range at 1940-2000 nm. These studies are usually *in vivo* and utilize a Yucatan mini or Yorkshire pig breed. Porcine models have been demonstrated to be a good substitute for human skin in laser exposure studies, with the Yucatan typically featuring a higher concentration of melanin granules in the epidermis compared to Yorkshire [5].

Cain *et al*. characterized the Yucatan porcine skin response to Er:glass lasers operating at 1540 nm for both long pulses of 600 µs and short Q-switched pulses of 31 ns [6]. They employed three different laser spot sizes for the long pulse case, measuring MVL ED_{50} 24-hour thresholds at 600 µs to be 20 J/cm^2, 8.1 J/cm^2, and 7.4 J/cm^2 for spot diameters of 0.7 mm (Gaussian, 1/*e*), 1 mm (Gaussian, 1/*e*), and 5 mm (tophat), respectively. In the case of the Q-switched short pulse of 31 ns, they determined an ED_{50} threshold of 6.1 J/cm^2 for a 5 mm diameter tophat beam profile.

Rico *et al*. also investigated porcine skin response to 1540 nm laser irradiation, but employed both the Yucatan mini and Yorkshire porcine models [7]. Using a pulse duration of 800 µs, they found the 24-hour MVL ED_{50} to be 128.3 mJ over a 0.62 mm beam diameter for the Yorkshire and 135.2 mJ over a 0.57 mm beam diameter for the Yucatan. These are equivalent to radiant exposure thresholds of 43.0 J/cm^2 for the Yorkshire and 53.5 J/cm^2 for the Yucatan. Roach *et al*. followed up this study with an additional data point using a 600 µs pulse over a 0.7 mm spot size, finding a radiant exposure threshold of 15 J/cm^2 [8].

There has been substantial work studying laser skin interaction close to 2000 nm. Chen *et al*. utilized a 2000 nm continuous-wave laser to determine Yucatan mini-pig skin damage threshold ED_{50}s to exposures of 0.25 s, 0.5 s, 1 s, and 2.5 s over beam diameters of 4.83 mm, 9.65 mm, and 14.65 mm [9]. The thresholds for each beam diameter fit very well to the power function $y = ax^{-b}$, where *y* is dose and *x* is the exposure duration. This function is a straight line on a log-log plot, and allows for prediction of dose thresholds at arbitrary exposure durations, so long as the thermal damage mechanism is consistent. They subsequently investigated the role of melanin in 2000 nm laser skin damage, performing exposures on subjects with both light and dark pigmented patches, and found minimal significant difference between the resulting radiant exposure ED_{50} thresholds [10]. Chen *et al*. also developed a computational model to reproduce temperature profiles and estimate damage thresholds from the experimental studies [11], as well as account for damage depths in tissue as seen in histology [12].

Oliver *et al*. performed a Yucatan porcine skin study at 1940 nm across a variety of beam diameters and exposure durations [13]. The 1940 nm wavelength is similar to 2000 nm, but with a slightly greater absorption coefficient in skin due to closer proximity to the local water absorption peak. Oliver *et al*. determined radiant exposure ED_{50} thresholds of 2.21 J/cm^2, 9.00 J/cm^2, and 22.3 J/cm^2 for a diameter of 0.48 cm and exposure times of 10 ms, 70 ms, and 10 s, respectively. They also found ED_{50}s of 2.95 J/cm^2 for a diameter of 1.0 cm and an exposure time of 50 ms, 2.93 J/cm^2 for a diameter of 1.8 cm and an exposure time of 70 ms, and 12.7 J/cm^2 for a diameter of 1.8 cm and

an exposure time of 10 s. Thermal profiles for this study were also reproduced using a similar computational modeling structure as Chen *et al*. [11].

The skin MVL thresholds from the 1540 nm, 1940 nm, and 2000 nm studies are graphed in Figure 3. These thresholds are all for continuous-wave, or single-pulse, exposures, with the MVL observed at 24 hours after irradiation and expressed in terms of average radiant exposure over the $1/e^2$ Gaussian beam diameter.

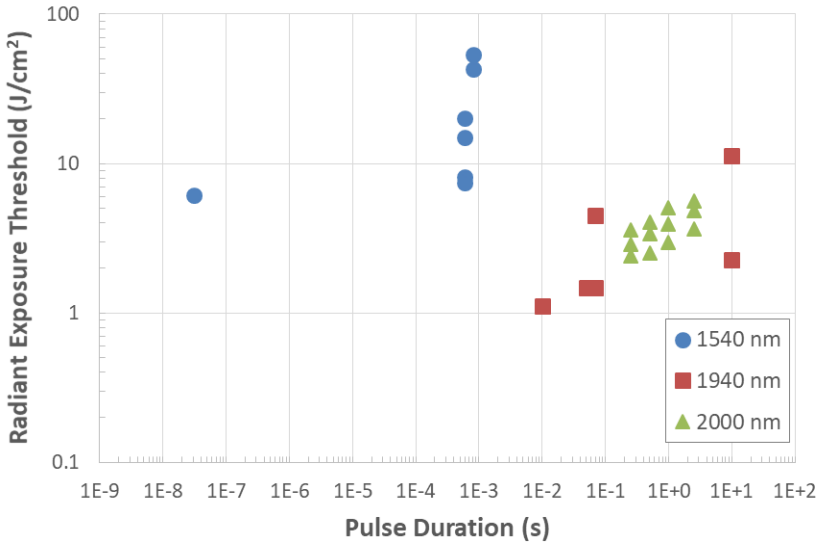

Figure 3. Skin MVL thresholds, 1400 nm to 2000 nm. Fiducial limits for these thresholds are available in the tables in Appendix A.

DeLisi *et al*. also explored Yucatan skin damage thresholds at the 1940 nm wavelength, but for the multiple-pulse cases using a pulse duration of 500 µs [14, 15]. Specifically, they looked at pulse trains of 20, 50, 100, 300, 1000, and 3000 pulses at pulse repetition frequencies (PRFs) of 100 Hz, 200 Hz, and 1000 Hz. The Gaussian $1/e^2$ beam diameter was 1.3 cm for the 20, 50, and 100 pulse cases, and 1.1 cm for the 300, 1000, and 3000 pulse cases. These multiple-pulse thresholds are plotted in Figure 4.

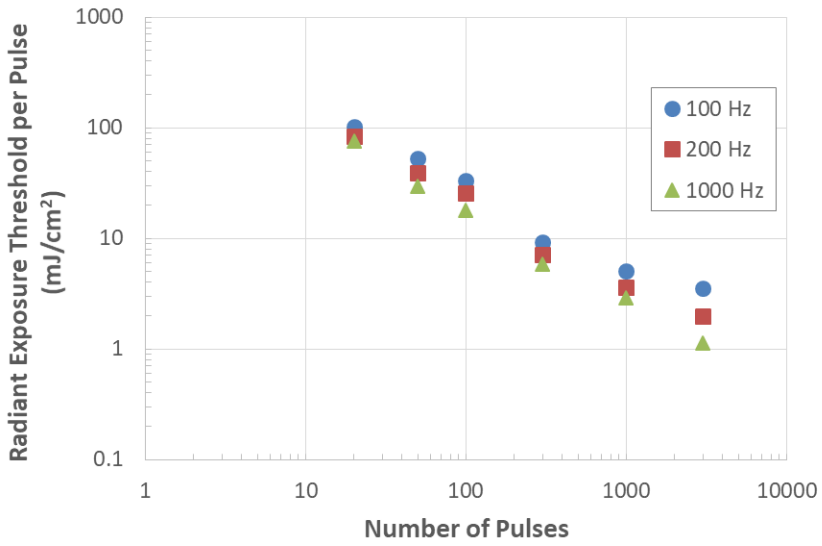

Figure 4. Multiple-pulse MVL thresholds at 1940 nm. Fiducial limits for these thresholds are available in the tables in Appendix A.

A compilation of the documented single-pulse skin laser damage thresholds between 1400 nm and 2000 nm is provided in Table A.1. The multi-pulse pulse skin laser damage thresholds at 1940 nm from DeLisi *et al*. [14, 15] are listed in Table A.2.

3.2 Supra-Threshold Skin Laser Injuries

Lasers have had wide application to the skin in medical contexts that could be considered supra-threshold. The most obvious of these applications is for cutting, where a laser is used as a substitute for a scalpel. These laser systems may not be excessively high in power, but they allow for very high irradiances due to a very small beam diameter. Laser cutting systems typically emit at wavelengths that absorb very highly in water, such as CO_2 lasers at 10,600 nm or Er:YAG lasers at 2940 nm. Pulses from these lasers will almost instantly vaporize the water within a cell, causing a micro-explosion with enough pressure to blow through the cell wall and carry the various solid components of the cell with it. Lower-absorbing lasers have also been used for surgical cutting, particular in highly vascularized tissue where there is a desire to coagulate blood vessels. However, surgical cutting lasers are not good examples of supra-threshold exposures from the context of dose response modeling, as their scale and mechanism of operation is on a nearly microscopic level.

Similarly, there are skin therapeutic techniques that could be considered as supra-threshold, such as fractional laser skin resurfacing, which sometimes involves ablating the outer epidermal layer to stimulate new collagen growth in the underlying dermis [16]. Complications of treatment can involve prolonged erythema, contact dermatitis, pigment alteration, and even hypertrophic scarring. Similar to surgical cutting lasers, these systems are designed to operate on a small scale, and undesirable effects are typically the result of suboptimal use during therapy.

In an early study, Hysell and Brownell performed experiments to determine correlation between gross and microscopic CO_2 porcine skin burns [17], utilizing routine haematoxylin and eosin (H&E) staining techniques. They found that as burns increase in severity macroscopically, there was a commensurate increase in microscopic evidence of tissue damage. However, there was also indication that burns from higher laser power densities produced more tissue damage than those from lower power densities, despite similar surface appearances.

Museux *et al*. investigated porcine skin burns after laser exposure, with histology and modeling for 808 nm and 1940 nm [18]. They did not restrict themselves to the MVL metric, but instead explored a variety of irradiance levels and exposure durations, recorded surface thermography, collected histology, and graded each exposure based on the degree of damage according to the French Society for Burn Study and Treatment (SFETB) classification guidelines. These grades are shown in Table 1. Museux *et al*. demonstrated that skin temperature was higher for 1940 nm than 808 nm at the same irradiance and exposure duration, as expected due to the higher water absorption at 1940 nm.

Table 1. SFETB classification for histology of skin burns

Histological grade	Description
1	Superficial epidermis involvement
2	Whole thickness epidermal involvement Basal membrane disruption Papillary dermis involvement
2+	Full-thickness epidermal necrosis, except for hair follicles Partial to complete basal membrane necrosis Reticular dermis involvement
3	Full-thickness epidermal necrosis, including hair follicles Complete basal membrane necrosis Deep dermis/hypodermis involvement

Zhang *et al*. performed a comparative study of laser-induced rat skin burns and thermal contact rat skin burns at the low-absorbing wavelength of 1064 nm [19]. They took histological sections of lesions and assessed wound healing using Masson's trichrome and picrosirius red staining, measuring the widths of epidermal necrosis and dermal denaturalization. They noticed that the dermal injuries induced by the laser were more severe 10 days after the exposure, while the skin burns induced by a hot soldering iron did not show a similar development or increased severity with the passage of time. These observations are consistent with the notion that low-absorbing, high-scattering 1064 nm radiation would deposit more heat deeper into the tissue before manifesting as a burn on the surface as compared to a contact burn, and thus damage a larger volume of tissue. Higher absorbing wavelengths would theoretically compare better to the metal contact skin burns, as they would similarly deposit most of their energy at the surface.

Schaffer *et al*. were also interested in comparative damage types to porcine skin, inducing a constant mid-dermal depth of injury by a dermatome (or scalpel) excision, a pulsed CO_2 laser operating at 10,600 nm, or a temperature-controlled metal template [20]. They harvested wounds after 5, 10, or 15 days and performed a variety of analytical tests to determine wound healing

mechanics, such as observing resurfacing differences, fibroblastic proliferation, capillary areas, and expression of three matrix metalloproteinases. The study concluded that although the three types of wounds undergo similar reparative processes, the magnitude and temporal sequences are very different amongst the modalities. Laser wounds in particular demonstrated the most fibroblast proliferation at day 5, but then evolved to have the least by day 10. Laser wounds also showed earlier peaks of capillary areas and metalloproteinase expression compared to contact burns.

In another study of comparative wounding effects, Ross *et al*. examined gross and microscopic effects of thermal and mechanical ablation devices to characterize immediate and long-term mechanisms in skin rejuvenation, specifically employing a dermabrader, dermatome, and several high-absorbing laser systems. These lasers included a 1 ms pulsed CO_2 (10,600 nm) laser with a 3 mm Gaussian beam diameter, a 1 ms pulsed CO_2 (10,600 nm) laser with a 0.2 mm Gaussian beam set to cover a 3 mm diameter in 0.2 s, and an Er:YAG (2940 nm) laser producing 1.5 J pulses with a 5 mm beam diameter. The group measured wound surface areas immediately after treatment, as well as at 2, 7, 17, and 60 days after treatment. They found that the CO_2 laser-induced wounds produced short- and long-term wound contraction that is greater than that induced by the purely ablative methods for the same total depth of injury, while the Er:YAG laser produced wound contraction profiles similar to those produced by mechanical wounding. This is perhaps due to the higher absorption coefficient in water at 2940 nm.

Fan *et al*. evaluated the recovery process of 1064 nm laser-induced porcine skin injury *in vivo*, examining several discrete irradiation doses over a 1 cm beam diameter and an exposure time of 0.5 s [21]. They determined an erythema threshold of 47.4 J/cm^2 and investigated exposures up to 608.3 J/cm^2, taking histological samples 0.25, 3, 7, 14, 21, and 28 days after exposure at select irradiation levels. A range of the macroscopically-visible supra-threshold skin injuries from this study are displayed in Figure 5. Histology demonstrated a high uptick in wound repair 7 to 14 days after irradiation, though doses beyond 126.4 J/cm^2 did not fully recover even at 28 days.

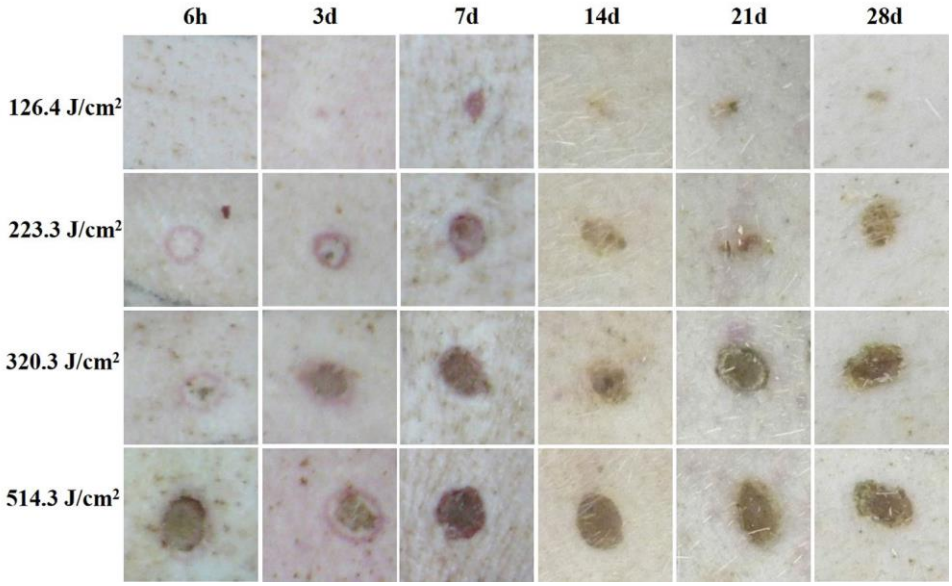

Figure 5. Macroscopic healing of skin at different times after four doses of 1064 nm laser radiation

In a follow-up study, Fan *et al*. investigated the use of optical coherence tomography (OCT) in quantitative and qualitative assessments of supercontinuum laser-induced rat skin injury [22]. The super-continuum laser spectrum ranged from 400 nm to 2400 nm and generated radiant exposure doses at 32.85 J/cm^2, 65.69 J/cm^2, 98.4 J/cm^2, and 197.1 J/cm^2 (exposure durations of 1, 2, 3, and 6 seconds, respectively), with an OCT system used to capture three-dimensional images as well as generate an optical attenuation coefficient (OAC) for the exposure region of interest. They found that the injured spots demonstrated increasing OAC values with the radiant exposure, though not necessarily proportional to the dose. The OACs and structural changes evident from three-dimensional visualizations indicated that the skin injuries were aggravated and the tissue repair trends weaken as the radiation doses increase.

Unlike several of the aforementioned studies, DeLisi *et al*. made an effort to quantify distinct degrees of various manifestations of supra-threshold damage in excised porcine skin [23]. This study employed a 1070 nm laser with Gaussian beam diameters of 0.3 cm and 0.7 cm to expose temperature-controlled excised porcine skin samples to a broad sampling of radiant exposure doses, while observing the tissue response with high-speed videography and thermography. Pulse durations were 3 ms for the 0.3 cm diameter and 100 ms for the 0.7 cm diameter. The exposure effects were sorted into three categories of progressively increasing severity based on observations from the high-speed video: permanent damage as evidenced by a persisting visible change after the laser exposure ended, formation of an epidermis steam bubble (or steam blister), and rupture of that epidermis steam bubble. Figure 6 is a photograph of these epidermis steam bubbles at the central cross section and overhead after exposure. The ED50 values and fiducial limits for each category of severity are in Table 2.

(a) (b)

Figure 6. Epidermis steam bubble, (a) central cross section and (b) overhead

Table 2. ED_{50} values and fiducial limits for supra-threshold endpoints of permanent damage, bubble formation, and bubble rupture, for 1070 nm laser exposure

Endpoint	Beam Diameter ($1/e^2$) (cm)	Pulse Duration (ms)	Radiant Exposure ED_{50} (J/cm^2)	Lower Fiducial (J/cm^2)	Upper Fiducial (J/cm^2)
Permanent damage	0.3	3	28.3	24.7	30.8
	0.7	100	95.5	74.2	105
Bubble formation	0.3	3	35.1	32.2	37.9
	0.7	100	141	130	152
Bubble rupture	0.3	3	49	45.6	52.3
	0.7	100	212	194	234

DeLisi *et al*. determined ED_{50} values and fiducial limits for each of these progressive damage occurrences and compared them to the current maximum permissible exposure (MPE) limits, MVL thresholds from Vincelette *et al*. [24], and ablation threshold approximations from a 1-D computational model [23]. These comparisons are graphed in Figure 7. This study provides quantifications for degrees of skin damage that are greater than the MVL level and thus considered to be supra-threshold, but it is unknown if these progressive damage definitions would hold for *in vivo* porcine skin.

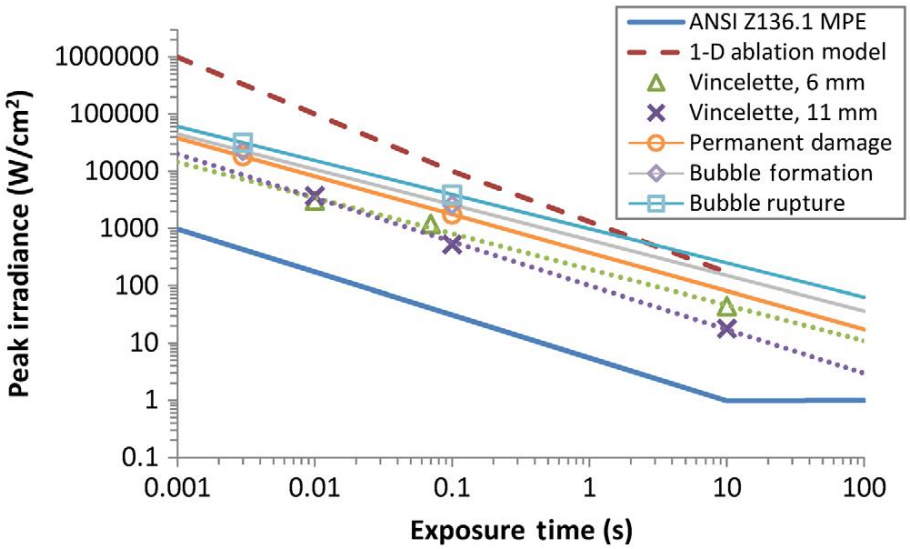

Figure 7. MPE limits, ablation onset threshold as calculated by a 1-D ablation model, MVL thresholds, and progressive damage occurrence ED_{50} values for 1070 nm laser exposure

The DeLisi *et al*. study utilized the endpoints of permanent damage, steam bubble formation, and steam bubble rupture due to the method of observation afforded by high-speed cameras [23]. However, supra-threshold injuries to skin are typically assessed by the medical community in terms of burn degrees, with definitions outlined in Table 3 [25]. These degrees are defined by penetration depth into the skin tissue. Noticeably, the definition of deep partial thickness 2nd degree burns is somewhat debatable, as that category can contain a broad range of clinical outcomes. Gibson *et al*. expound upon this topic in a multi-institutional collaborative effort, developing a more complex but consistent rubric for analyzing deep partial thickness porcine skin burns that takes into account a finer segmentation of the dermis, as well as the intensity of the damage [26].

Table 3. Burn degrees

Type	Layers involved	Appearance	Healing Time	Prognosis and Complications
1st degree, superficial	Epidermis	Red without blisters	5-10 days	Heals well. Repeated sunburns increase the risk of skin cancer later in life.
2nd degree, superficial partial thickness	Extends into superficial (papillary) dermis	Redness with clear blister. Blanches with pressure.	2–3 weeks	Local infection (cellulitis) but no scarring typically
2nd degree, deep partial thickness	Extends into deep (reticular) dermis	Yellow or white. Less blanching. May be blistering.	3–8 weeks	Scarring, contractures (may require excision and skin grafting)
3rd degree, full thickness	Extends through entire dermis	Stiff and white/brown. No blanching.	Prolonged (months) and incomplete	Scarring, contractures, amputation (early excision recommended)
4th degree	Extends through entire skin, and	Black; charred with eschar	Does not heal;	Amputation, significant functional impairment and in some cases, death.

	into underlying fat, muscle and bone		Requires excision	

Defining supra-threshold skin injuries in terms of damage to skin layers is conducive to a computational modeling approach. Current validated simulations of skin thermal response and threshold damage prediction allow for definition of skin layers and can track thermal profiles at arbitrary depths within a given layer [27]. While these models have been typically deployed to reproduce the MVL damage thresholds by applying the Arrhenius integral on the skin surface or at some point within the epidermis [11, 12, 27], they can easily be extended to calculate damage extension into the layers of the dermis and subcutaneous fat that define various burn degrees. A similar approach was employed by Lyu *et al*. to determine thresholds for limiting reversible damage while maximizing an aversion response [28].

4.0 CORNEA

The human cornea is a ~ 600 µm thick avascular tissue that forms the anterior surface of the eye. It is transparent and is the primary refractive element in the eye. The cornea consists of 5 distinct tissues arranged in layers as shown in Figure 8. Starting from the anterior layer, they are: the epithelium (~ 50 µm thick), the Bowman's layer (8 -12 µm thick), the stroma (~ 500 µm thick), the Descemet's membrane (2 - 10 µm thick), and the endothelium (5 µm thick). The corneal epithelium is covered in tear film (3 - 8 µm thick), which consists of lipid, aqueous, and mucin layers although 98% of its total volume is water.

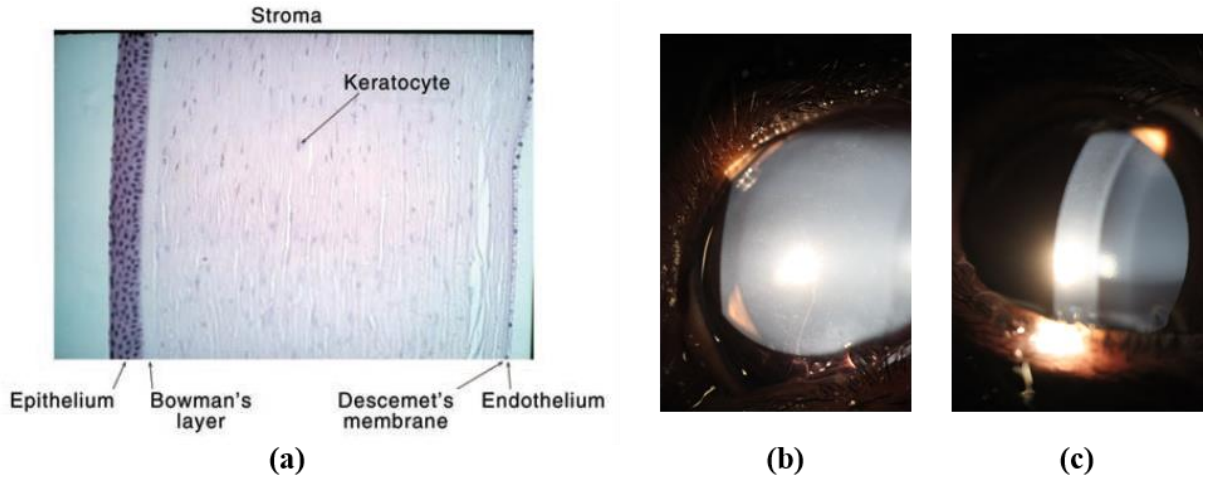

Figure 8. (a) Light micrograph showing a cross section of the human cornea. The various layers from anterior (on the left) to posterior (on the right) are the epithelium, showing dark-stained cell nuclei; the Bowman's layer; the stroma, showing keratocytes between its layers; Descemet's membrane; and the endothelium [29]. Slit lamp photograph of a normal Dutch Belted rabbit cornea with dilated pupil under (b) wide beam illumination and (c) optical section.

The *corneal epithelium* consist of three different cell types (squamous, wing, and columnar cells) forming around 6 cell layers. It is a self-renewing tissue such that all the cells turnover within 7 to

10 days. This process occurs as new cells form in the basal cell layer via mitosis and migrate towards the outer surface of the cornea, replacing the squamous cells, which are shed into the tear film. When an injury occurs, this cell turnover accelerates and the epithelial cell layer heals within 1 to 3 days. The *Bowman's layer* consists of a random arrangement of type I and type II collagen fibers but does not regenerate following injury. However, lesions to the Bowman's layer do not appear to affect vision. The *stroma* forms the bulk of the cornea and consists of densely packed, parallel laminar collagen fibrils and corneal keratocytes. When a corneal injury occurs, the corneal keratocytes undergo apoptosis or become involved in the healing process. The stroma has a slow and limited repair capacity and any remaining scars may have an effect on the subject's vision. The *Descemet membrane* consists of type VIII collagen produced by the neighboring endothelial cells. It is highly resistant to trauma and can regenerate if damaged. The *endothelium* consists of a single layer of cells separating the cornea from the anterior chamber filled with aqueous humor. The endothelial cells cannot divide so they cannot regenerate when damaged. However, the undamaged cells have some ability to change shape or size to restore the integrity of the endothelium after an injury.

One of the objectives of this literature review was to identify measures of severity of outcome to corneal tissue from exposure to a strongly absorbing laser (1400 nm to 2000 nm). This is not a straightforward task given that the reports found in the literature utilize a variety of different experimental setups used to produce corneal tissue damage as well as a large range of experimental conditions, including laser sources and exposure parameters, human *vs*. animal models, live *vs*. excised corneas, among others [30]. In addition, there is no consensus on the definition for damage, although three regimes can be identified from published data. Lesions generated by an exposure level that results in a minimum visible lesion (MVL) are referred to as threshold lesions and typically appear within 1 h from exposure [31, 32]. Threshold lesions appear as greyish white spots on the cornea and can be detected with a slit lamp down to 100 μm in diameter [33]. According to Jean *et al*. [32], if the lesion is visible immediately after exposure, that level of exposure is considered a "super-threshold" exposure. Note that, given the typical procedure used to determine corneal damage thresholds, or ED_{50}, most threshold studies include data within the super-threshold, or supra-threshold, exposure regime as defined by Jean *et al*. [32]. Therefore, some of the summaries in Section 4.1 include lesion characterization for supra-threshold exposures. As the irradiation fluence increases, material is removed and endpoints of exposure transition from tissue damage to ablative tissue removal [30]. For the purposes of this technical note, we will consider that supra-threshold exposures include superficial lesions of the cornea visible immediately after exposure, which may heal in a few days, as well as more invasive lesions that result in corneal ablation. In addition, we will include exposure conditions where more than one ocular component is affected, *e.g*. the cornea and the lens. Section 4.2 contains summaries of studies that explicitly characterize supra-threshold lesions as defined in this manner at wavelengths close to the infrared, with section 4.2.2 primarily focused on studies to determine the ablation threshold. In the following summaries, we will focus on the results for cornea or cornea models, that is, we will omit the results for other tissues even if included in the publication that is summarized.

4.1 Cornea Laser Damage Thresholds From 1400 nm To 2000 nm

Current published damage threshold data for wavelengths between 1400 nm and 2000 nm are limited to the following wavelengths: 1410 nm [34], 1540 nm [33, 35-42], 1550 nm [43], 1573 nm [44], 1732 nm [45], and 2000 nm [46]. Most of the damage threshold data reported in the studies summarized in this section was used in Jean *et al*. to validate their computer model to predict cornea injury thresholds for wavelengths between 1050 nm and 10.6 µm down to the nanosecond regime [32]. Jean's model incorporates the optical properties of the cornea, including the tear film, transient increases in temperature, and a temperature dependent rate of reaction that, when integrated over time, causes damage. The results from Jeans' model compare well with most of the experimental data currently available in the literature and summarized below.

Archibald and Taboada reported an ED_{50} of 2.42 J/cm^2 for 1410 nm and a 25 ns pulse duration obtained from rabbit corneas using a 1.09 mm diameter beam [34]. This value is much lower than expected when compared to other experimentally determined damage thresholds in the 1200 nm to 1500 nm range scaled by the water absorption coefficient or those obtained from computational models [47].

There are multiple articles reporting on *in vivo* damage thresholds at 1540 nm with pulse durations between 100 s and 0.8 ms [36-38, 41, 42], but only two reports for nanosecond pulse durations, one in rabbits (40 ns) [36] and the other one in monkeys (50 ns) [35]. There is a gap in the data for pulse durations between 800 µs and 50 ns.

Avdeev *et al*. used an erbium laser at 1540 nm to obtain the ED_{50} in chinchilla rabbit corneas using 1 ms long pulses and, operating in the Q-switch regime, 40 ns long pulses [36]. In both cases, the laser emitted in the lowest mode and had a Gaussian beam profile. The authors used a lens placed at a distance $d < f$ such that the spot size on the cornea was between 1 mm and 2 mm. They determined that the ED_{50} damage threshold was 7.2 ± 0.6 J/cm^2 for the 1 ms pulse durations and 4.7 ± 1.2 J/cm^2 for the 40 ns pulse durations.

Lund *et al*. obtained the ED_{50} in owl monkeys using a Q-switch erbium laser emitting 50 ns long pulses at 1540 nm [35]. Two different focusing geometries were used: an approximately 2 mm diameter beam and a focused beam. No corneal damage was observed with the collimated beam and energy densities ranging from 0.1 J/cm^2 to 1.0 J/cm^2. The focused beam was approximately Gaussian and the diameter was determined from the 1/*e* intensity points to be ~0.57 mm diameter focal spot. The criteria for a minimum visible lesion was a corneal lesion seen by slit lamp 1 h post exposure although they were examined immediately, 0.5 h, and 1 h post-exposure. Some subjects were observed at 1 day, 7 days, and 3 weeks after exposure. Near-threshold lesions showed a shallow depression of the epithelial surface. More severe lesions showed a white opacification that extended into the stroma and, sometimes, wrinkling of Descemet's membrane. The injuries healed in 1 to 3 days but the stromal opacification remained up to 3 weeks. Histopathological analysis of fresh corneal lesions showed localized coagulation necrosis of the epithelium, Bowman's membrane, and anterior stromal layers. Lesions that healed did so through proliferation of the corneal epithelium with the formation of a collagenous scar in the anterior stroma. The 50% probability of corneal damage obtained was 21 J/cm^2 where all exposures at energy densities larger than 30 J/cm^2 produced injury. No injuries were detected for energy densities below 17 J/cm^2.

In a series of publications, Johnson *et al*. and Roach *et al*. investigated *in vivo* and *in vitro* cornea exposure thresholds to 0.8 ms single pulses from a 1540 nm erbium laser [38, 39, 48]. For the *in vivo* study, they exposed corneas from Dutch belted rabbits to a 0.002 cm^2 spot size diameter at the focus of a lens, where the focal point was determined from the $1/e^2$ intensity points using the knife edge technique. Each cornea received an individual marker lesion to aid in locating the injuries and three additional exposure energies. The authors conducted ophthalmoscopic and slit lamp examinations at acute, 1 h and 24 h post exposure. Lesions were clearly visible immediately after exposure, *i.e*. acute exposure examination, and no additional lesions were identified upon ophthalmoscopic or slit lamp examination. Under the slit lamp, all lesions had sharp edges, were well demarcated, and showed no apparent damage outside of the main lesion. They appeared to be limited to the stroma and did not heal within 24 h. Acute histological examinations using H&E staining showed that damage to the epithelial cells was distended by the underlying stromal injury, which did not extend to the endothelium. The authors used probit analysis on the 24 h post exposure data to obtain an ED_{50} of 56.7 J/cm^2, where the lower and upper fiducial limits were 54.9 J/cm^2 and 58.9 J/cm^2 at 95% confidence. Note that, based on Jean's definition, these studies fall within the super-threshold exposure category [32].

For the *in vitro* portion of the studies, Johnson *et al*. and Roach *et al*. utilized a corneal equivalent (CE) model produced from rabbit corneal tissue [38, 39, 48]. The CEs were grown in transwell containers and consisted of a single endothelial bed overlaid with stromal collagen, fibroblasts, keratocytes, and epithelial cells, forming a layered structure. Transwells were removed from the tray for laser exposures and each transwell received a single exposure. They were placed 25.4 cm from the focusing lens, resulting in an average elliptical area of 0.003 cm^2. Acute lesions were clearly visible upon examination and resulted in an ED_{50} of 83.7 J/cm^2 where the lower and upper fiducial limits were 80.5 J/cm^2 and 90.6 J/cm^2 at 95% fiducial limits. After exposure, the CE's were cold packaged and shipped for histology and genomic expression studies. *In vivo* corneas and CE's showed extensive damage to collagen in the stroma, specifically, vacuolization between the lamellar sheets of collagen fiber. Denaturation of the stroma appears to be present throughout the damaged area. Although the histological findings for the *in vivo* corneas and CE's are similar, the results for the ED_{50} do not overlap, therefore it is unclear if the CE's are a reasonable model for determining damage thresholds. This is particularly important for wavelengths that are highly absorbed by water, where the presence or absence of a tear layer plays a larger role.

Stuck *et al*. measured the ED_{50} of rhesus macaque corneas exposed to a single pulse at 1540 nm [33, 37]. The laser's emission lasted 1.6 ms but was 930 μs at the half-power points. The beam was approximately Gaussian and the effective irradiance diameters were reported at the $1/e$ intensity points. The authors used two focusing geometries, an unfocused 2.1 mm diameter beam and a focused 1 mm diameter beam. For the unfocused beam, a total of 25 exposures were made with a dose ranging from 2.1 J/cm^2 to 5.3 J/cm^2. No lesions were observed during or after the exposures. In the focused geometry, two to 12 exposures were placed on each eye and the response criteria was the observation of an opacity or lesion using a slit lamp. The lesions were examined 1 h and 24 h after exposure and some up to 10 months after exposure. The diameter and depth of the lesion increased as the dose increased. Lesions had a conical shape when looking at the cross section and involved between ½ to the full corneal thickness. Some near threshold exposures resulted in lesions that persisted, indicative of stromal scarring while lesions exposed to ~1.5 ED_{50}

presented spoke-like stromal scars radiating away from the central lesion. The ED_{50} was 9.6 J/cm^2. In this study, the authors also determined the ED_{50} at 1064 nm, 1318/1338 nm, and 2060 nm.

In a series of studies, McCally *et al*. determined the damage threshold at 1540 nm for exposure durations ranging from 0.036 s to 0.260 s for a 0.1 cm beam [41], for exposure durations ranging from ~1 s to 100 s for 1/*e* beam diameters of 0.05 cm to 0.70 cm [40], and multiple pulses [42]. For these studies they utilized an erbium fiber amplifier driven by a laser diode. The laser emits in the TEM_{00} mode. The output beam diverges, therefore it was collected with a 63 mm focal length biconvex lens and the cornea was positioned past the focal point. The beam was visualized on a fluorescent screen and was determined to be Gaussian at the location of the cornea. The knife-edge technique was used to obtain the 1/*e* beam diameter and a shutter controlled the exposure durations. The authors utilized New Zealand white rabbits and positioned the eyes so that the incident beam was perpendicular to the central cornea. Thirty minutes after exposure, the subjects were sacrificed and the eyes were examined for damage with a slit lamp microscope. The criteria for damage was "a superficial, barely visible, gray-white spot," see Figure 9. Since there was very little overlap between exposures that produced damage and those that did not, the authors did not use probit analysis to determine the ED_{50}. Instead, they defined the injury threshold as the center of the bracket between an exposure that produced a minimal lesion and one that did not. For exposure durations shorter than 1 s, the beam diameter was 1 mm. The damage thresholds found under those conditions were 6.62 J/cm^2 for 0.036 s, 8.40 J/cm^2 for 0.056 s, 10.4 J/cm^2 for 0.110 s, and 14.6 J/cm^2 for 0.255 s. For 1.04 s exposure durations, the damage thresholds were determined for 0.5 mm, 1 mm, 2 mm, and 5 mm beam diameters, resulting in 70.1 J/cm^2, 32.3 J/cm^2, 14.7 J/cm^2, and 12.8 J/cm^2, respectively. For 2.05 s exposure durations, the damage thresholds were determined for 0.5 mm, 1 mm, 2 mm, and 7 mm beam diameters, resulting in 116 J/cm^2, 59.4 J/cm^2, 28.9 J/cm^2, 18.9 J/cm^2. Similarly, for 11 s exposure durations, the resulting damage thresholds were 367 J/cm^2, 158 J/cm^2, 79.3 J/cm^2, and 40.3 J/cm^2. The damage thresholds for 100.0 s exposure durations for 2 mm and 7 mm diameter beams were 370 J/cm^2 and 137 J/cm^2. The near threshold lesions for 1.04 s exposures with nominal beam diameters of 2 mm and 5 mm had sharply defined edges and looked uniform from edge to edge as opposed to appearing as a diffuse spot such as for the other exposure conditions. The authors also looked at long exposure durations (100 s) at sub-threshold levels (0.7 and 0.08 times the damage threshold) to a 0.7 cm diameter beam but found no evidence of damage up to 48 h after exposure. We have not included a summary of results for the multi pulse experiments.

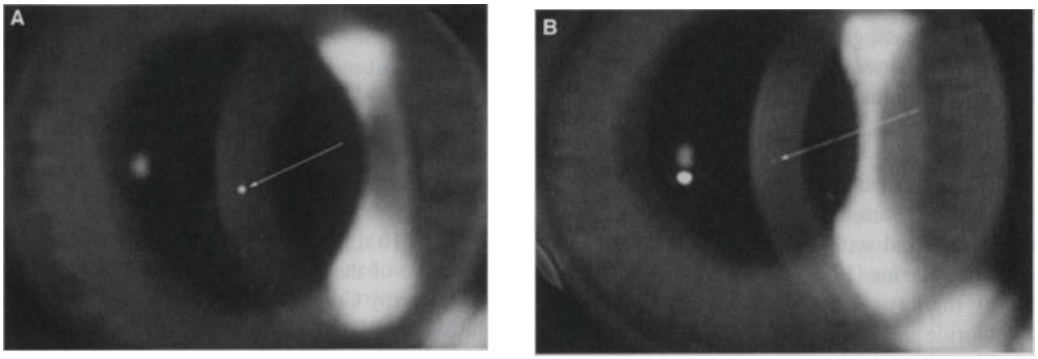

Figure 9. Slit lamp photograph of a normal Dutch Belted rabbit cornea showing lesions produced by 0.11 s exposures at 1540 nm with a beam diameter of 0.1 cm. (a) Radiant exposure of 15.3 J/cm^2 or 1.47 times the damage threshold. (b) Radiant exposure of 10.8 J/cm^2 or 1.038 times the damage threshold.

Ham and Muller used Dutch belted rabbits to determine the damage threshold produced by a diode laser centered at 1550 nm [43]. They used exposure durations of 1 s, 10 s, and 100 s with a beam diameter of approximately 1.85 mm. An electronic shutter controlled exposure durations. A slit lamp was used to identify the injuries immediately post exposure; acute examination, and every 24 h afterwards for 2 weeks. Damage was not observed immediately post exposure for any condition studied. Exposure durations of 1 s and 10 s did not produce damage between 0.62 mW and 5.62 mW (0.5 mW increments). Exposure durations of 100 s did not produce damage between 0.62 mW and 4.1 mW (0.5 mW increments). At 4.6 mW a minimal lesion was observed at 24 h post exposure. In the second part of the study, the authors exposed the cornea for 100 s and increased the power in 0.2 mW increments, starting at 4.0 mW. They conclude that 4.2 mW produces a transient effect that is detected 24 h post exposure but disappears in 48 h. The authors of this study devised a grading system for injuries based on the appearance and size of the lesions and how long they took to heal. It ranged from Grade 0 – *No effect* to Grade 5 – *Partial loss epithelial cell layer, treated with chloromycetin ointment, healed in 2 wks*. These results are in disagreement with other studies of threshold damage in that the effects do not appear until 24 h post exposure and the estimated temperature rise is much lower than would be expected for a thermal mechanism [41].

Courant *et al*. evaluated the *in vivo* and *in vitro* corneal damage threshold induced by 1573 nm laser radiation produced by a pulsed Nd:YAG laser and an optical parametric amplifier which delivered 3 ns long pulses [44]. The beam had an approximately top-hat profile. For the *in vivo* study, they delivered single pulses with a beam diameter of 400 μm to Fauve de Bourgogne rabbit corneas using a lens with a 100 mm focal length. To aid in locating the lesions, they placed marker lesions (consisting of 5 to 10 pulses) flanking an individual single pulse exposure. The authors performed clinical evaluations using a slit lamp and a surgical microscope 30 min, 24 h, and 7 days after exposure and used fluorescein to identify near threshold lesions. The criteria for a minimal visible lesion was a "very small shallow depression of the epithelial surface with slight fluorescein staining when observed using the blue filter in the surgical microscope". A discrete opacity or a small white point was considered a more severe lesion. Near threshold lesions were hard to detect after 24 h while others had disappeared. After 48 h, no lesions could be detected and

after 7 d, most marker lesions had disappeared. The corneas of a few subjects were extracted at 1 h, 24 h, and 48 h, fixing and sectioning them before staining them with orcein or H&E prior to being examined with a light microscope. For corneas fixed 1 h post-exposure, the damage appeared to be confined to the epithelium and a small part of the stroma. The injury was approximately 100 µm in diameter. For low radiant exposures, the lesions were hard to detect clinically. The histological analysis showed that for a radiant exposure of 16.7 J/cm^2, the epithelium was damaged, *i.e*. "disrupted and roughened," with few cells gone. However, the damage was not uniform and did not have a well-defined edge. In addition, large vacuoles were observed in the stroma, down to a depth of 50 µm. No long-term effects were observed. The data was processed using probit analysis where the number of exposures was 84. They obtained an ED_{50} of 26.6 J/cm^2 (4.3 J/cm^2 if calculated with a 1 mm beam diameter). The lower and upper fiducial limits were 23.5 J/cm^2 and 30.4 J/cm^2 at 95% confidence and the slope S was 1.4 ($S = ED_{84.1}/ED_{50} = ED_{50}/ED_{15.9}$). For a radiant exposure of 30.55 J/cm^2, histological analysis showed that the epithelium was gone over a 400 µm to 500 µm diameter and the stromal fibers appeared to be disturbed down to half of the corneal depth as shown in Figure 10. However, the authors speculate that the damaged epithelium could have been removed during the fixation process.

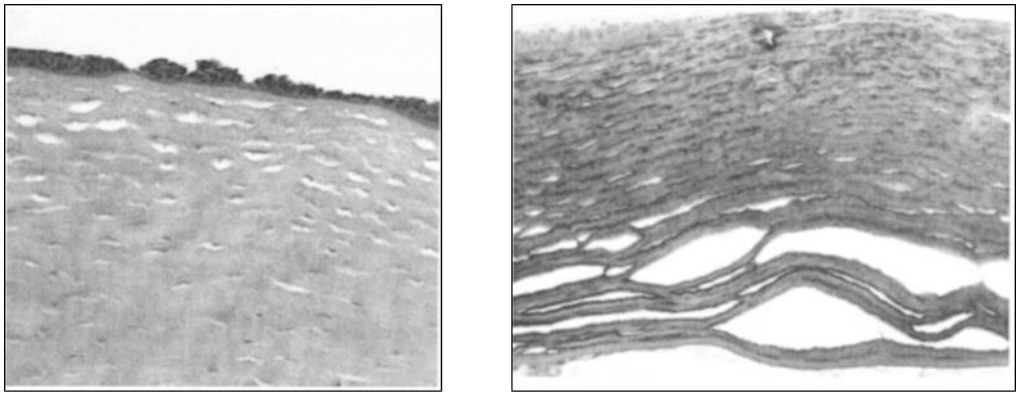

Figure 10. Light micrographs of histological sections. (a) Through the center of a lesion produced by a 3 ns pulse at 1573 nm with a radiant exposure of 16.7 J/cm^2 (below threshold). The beam diameter was 400 µm. Tissue was fixed 1 h after exposure. Epithelium is disrupted and roughened. Large vacuoles are present in the anterior stroma. (b) Of the border of a lesion induced by a 3 ns pulse at 1573 nm with a radiant exposure of 30.55 J/cm^2 (1.15 times the damage threshold). The beam diameter was 400 µm. Tissue was fixed 1 h after exposure. The epithelium is highly disrupted and epithelial layer have disappeared.

In the *in vitro* study performed by Courant *et al*., the authors used a) human primary keratocytes and b) rabbit primary keratocytes obtained by enzymatic dissociation and scraping, and c) an HT 1080 epithelial cell line from human fibrosarcoma from ATCC [44]. Cells were cultured and seeded in 96 well plates in order to perform laser exposures and study cell proliferation, senescence, and cytotoxicity. Cells were also placed in a chamber slide system to perform morphological analysis and detect apoptosis. All evaluations were performed using established techniques in molecular biology using commercially available kits. Individual wells were located past the focal point of a 100 mm focal length doublet such that the laser beam was 3.5 ± 0.3 mm in diameter, fully illuminating the bottom of the well. The authors used 3.8 mJ pulses with a pulse

duration of 3 ns, a repetition rate of 10 Hz and 13, 27, or 40 pulses. This resulted in a total energy of 0.5 J, 1 J, or 1.5 J and radiant exposures of 5.1 J/cm^2, 10.6 J/cm^2, or 15.9 J/cm^2. The chamber slides were also placed past the focus of the lens such that the beam diameter was 6 ± 0.5 mm. Cells were irradiated with a repetition rate of 10 Hz and 30, 60, or 90 pulses for a total energy of 1.1 J, 2.2 J, or 3.3 J, respectively. This corresponds to radiant exposures of 3.9 J/cm^2, 7.9 J/cm^2, and 11.8 J/cm^2. Cell proliferation and cytotoxicity of senescent cell did not show any effects due to laser irradiation. However, the number of mitotic and apoptotic cells was different between irradiated cells and control cells with a decrease in mitotic events and an increase in apoptotic events 28 h after exposure. At 48 h after exposure, this trend continued for the lower two exposure doses but inverted for the 15.9 J/cm^2 radiant exposure. Morphological abnormalities, including apoptotic bodies, were observed at 28 h post exposure for all doses. The increase in apoptosis was quantified using apoptotic markers and was extremely dose dependent, being apparent even at the lowest dose of 3.9 J/cm^2. From these studies, the authors conclude that clinical evaluations are insufficient to unambiguously determine the damage thresholds given that they only provide a rough and superficial evaluation of the injuries.

Stuck *et al*. measured the rhesus macaque corneal response to an erbium laser operating at 1732 nm for 225 µs (FWHM) long emissions that reached full extinction at 380 µs [45]. The laser beam was focused onto the corneal plane with four different lenses, which provided a range of corneal irradiance diameters and used neutral density filters to adjust the energy per exposure. The intensity profiles were approximately Gaussian and are reported at the 1/*e* intensity points. The authors examined the corneas with a slit lamp biomicroscope immediately after exposure, 1 h, 24 h, 48 h, 1 week, and up to 6 months after exposure. The corneal lesions generally involved the entire corneal thickness and some disappeared by the 48 h evaluation. The authors used probit analysis to determine an ED_{50} of 29 J/cm^2 (95% confidence interval 27 J/cm^2 to 31 J/cm^2) with a slope of 1.30 for a 515 µm beam diameter, 26 J/cm^2 (23 J/cm^2 to 29 J/cm^2) with a slope of 1.34 for a 740 µm beam diameter, and 22 J/cm^2 (20 J/cm^2 to 23 J/cm^2) with a slope of 1.28 for a 920 µm beam diameter. From these results, the authors conclude that the radiant exposure needed to produce a corneal lesion decreases as the beam diameter increases.

Chen *et al.* used Dutch Belted rabbit corneas to determine the ED_{50} at 2000 nm for continuous wave (CW) 0.1 s, 0.25 s, 0.5 s, 1 s, 2 s, and 4.0 s exposure durations [46]. They utilized a thulium fiber optic CW laser and an iris shutter system to control the exposure duration. The authors used telescopes to collimate the beams. The laser beam profiles were nominally Gaussian with 1/e^2 diameters of 1.17 mm and 4.02 mm measured using a beam profiler and the knife-edge technique. Note that the average radiant exposures reported were calculated as the laser energy divided by the 1/e^2 spot area. Initial lesion determinations were done by two readers immediately after exposure using an overhead surgical light, in addition a slit lamp exam was conducted approximately 1 h after irradiation. Lesion scores were "superficial damage minimally visible without magnification," "readily apparent lesion on surface with some circular symmetry," and "severe lesion, circular symmetric opacity with shrinkage of epithelium at the center." IR videos were recorded and utilized to obtain a temperature map of the corneal surface during exposures. For select exposure conditions, a 24 h slit lamp exam was also conducted. The criteria for a minimum visible lesion was "a superficial surface whitening" at 1 h post exposure. At threshold, the lesion diameters were smaller than the beam diameter and ranged in diameter from 0.3 mm to 0.6 mm for the 1.17 mm diameter beam and 0.8 mm to 1.1 mm for the 4.02 mm spot size. Some of the

threshold lesions were still visible at the 24 h examination. The authors determined the 1 h post exposure ED_{50} threshold power for all 12 exposure duration and spot size conditions using probit analysis. For a 1.17 mm spot size, the authors found ED_{50} threshold powers (probit slopes) equal to 236.1 ± 2.7 mW (200.3) for 0.1 s pulse durations, 154.1 ± 3.6 mW (200.8) for 0.25 s pulse durations, 116.5 ± 1.1 mW (250.1) for 0.5 s pulse durations, 114.9 ± 5.1 mW (52.4) for 1 s pulse durations, 87.6 ± 1.9 mW (211.2) for 2 s pulse durations, and 73.2 ± 0.8 mW (217.7) for 4 s pulse durations. For a 4.02 mm spot size, the authors found ED_{50} threshold powers (probit slopes) equal to 2272.8 ± 45.2 mW (115.1) for 0.1 s pulse durations, 1209.0 ± 23.1 mW (120.3) for 0.25 s pulse durations, 788.1 ± 5.5 mW (328.7) for 0.5 s pulse durations, 538.2 ± 60.8 mW (20.3) for 1 s pulse durations, 402.4 ± 48.6 mW (19.0) for 2 s pulse durations, and 303.6 ± 3.5 mW (207.6) for 4 s pulse durations. In general, they had small standard deviations of threshold powers, close lower and upper fiducial limits, and large slopes. The resulting damage threshold follow an empirical power-law relationship (proposed by McCally *et al*. [29]) between the threshold radiant exposure H and the exposure duration t of the form $H = at^b$, where a and b are positive coefficients obtained by fitting the experimental data. Temperature measurements showed that the corneal temperature response is proportional to the radiant energy and as the laser exposure duration increases, more energy is required to induce a visible lesion. The radiant exposure needed to produce a corneal lesion decreases as the irradiance diameter increases. The authors reported that as they increased the laser power beyond threshold, they saw readily apparent surface lesions with somewhat circular symmetry. At powers ~1.5 times the ED_{50}, the lesions were more severe with circular symmetric opacity and shrinking of the epithelium at the center of the injury. In the latter case, dehydration and coagulation of corneal epithelium as well as denaturation of corneal stroma occurred.

4.2 Supra-Threshold Cornea Laser Injuries

4.2.1. Pre-ablative supra-threshold effects

In a study by Zuclich *et al*. [49], the authors used a CW Nd:YAG laser to produce either 1.318 μm or 1.356 μm in order to study ocular effects at supra-threshold energies on the cornea and retina. An electronically controlled mechanical shutter was used to select the exposure duration. The authors utilized rhesus macaques and Dutch Belted rabbits. Prior to any laser exposure, the subjects were examined with a slit lamp, fundus camera, fluorescein angiography, baseline photograph taken at the fundus camera, and refraction to the nearest 0.25 diopter. For rabbits whose anterior ocular tissue would be exposed, only the slit lamp and fundus camera were used during the examinations. For exposures to the anterior ocular tissues, the laser beam was focused to a 1.0 mm (0.7 mm) diameter spot at the corneal plane and was normally incident at 1318 nm (1356 nm). Given the beam's divergence, it was considered as collimated. For retinal exposures, the subject was placed on an adjustable stage in front of a fundus camera. A sliding gold mirror was placed in front of the fundus camera so that, when the mirror was in place, the laser beam was collinear with the optical axis of the camera. When the mirror was out, the fundus camera had an unobstructed view of the fundus. The laser beam had a 5.0 mm beam diameter at the corneal plane and was considered to be collimated. For rhesus macaques, marker lesions on the retina were placed outside of the pigmented macula in a grid pattern to mark subsequent IR laser exposures. For rabbits, marker lesions were placed below the visual streak. After each exposure session, each exposure

site was scored based on the presence or absence of a lesion 1 h post-exposure in addition to subsequent examinations for up to 3 months for some subjects. Note that some lesions did not appear until several days post exposure and sometimes took longer to reach maximum expression, including degeneration of tissues other than that directly irradiated by the laser. The following two paragraphs summarize the results obtained for 1318 nm and 1356 nm respectively.

At 1318 nm, subjects were exposed for times ranging between 0.2 s and 1 s for corneal effects and up to 20 s for retinal effects. The corneal spot size diameter was 1.0 mm when irradiating the anterior ocular tissue and 5.0 mm when irradiating the retina. In some cases, laser induced damage was observed in the cornea, lens, and iris of rhesus macaques. A similar array of lesions was observed in rabbits with the addition of retinal damage. The cornea damage threshold in rabbits was 175 J/cm^2 while in the rhesus macaques it was 72 J/cm^2 (1 h readings). Exposure to doses slightly larger than the cornea damage threshold resulted in highly reflective spots observed immediately following exposure where the lesions were full-thickness. At 48 h post threshold exposures, the epithelial damage had been repaired but a stromal lesion, usually with a smaller diameter than the initial epithelial lesion, was observed together with an endothelial lesion with a diameter equal or slightly larger than the initial epithelial lesion. Both rabbits and rhesus presented stromal and endothelial effects for almost every instance of initial epithelium damage. In rhesus, several threshold exposures showed a minimal endothelial effect at 48 h even though no corneal lesion had initially been observed. Changing those points from no-lesion to lesion changes the cornea damage threshold for rhesus to ~50 J/cm^2 (48 h reading). Stromal and endothelial lesions remained longer than corneal epithelial effects. However, lesions produced slightly above threshold healed within several weeks post exposure. Lesions produced by doses 2 to 3 times threshold or higher remained throughout the duration of the study and represents permanent corneal scarring. At supra-threshold doses, the authors also detected cataracts directly behind the corneal lesions and determined the threshold for cataract induction to be 260 J/cm^2 incident at the cornea for both rabbits and rhesus. The cataracts produced by threshold level exposures appeared as two discrete lesions; one located at the capsule (anterior surface cataract), or just sub-capsular, and the second one located directly behind but away from the capsule (cortical cataract), involving as much as one third of the lens thickness. The latter appeared to show tapering of the lesion diameter with increasing depth. For exposures slightly above threshold, the anterior surface cataract resolved within a few weeks while the cortical cataract remained. Cataracts produced by 2 or more times threshold remained for several months and are assumed to reflect permanent lens damage. The authors also illuminated the iris of undilated eyes and were able to observe anterior surface cataracts directly beneath the projected irradiated spots, referred to as indirect cataract. The threshold for indirect cataract induction was ~130 J/cm^2 incident at the cornea. With supra-threshold exposure doses, the diameter of the indirect cataract was significantly larger than the cataract formed by irradiating the lens with the same exposure. In addition, the iris would not dilate for several days post exposure and, in a few cases, a perforation of the iris was observed at several weeks post exposure. To study retinal effects, the retina was illuminated for up to ~20 s with a 5.0 mm diameter beam. No retinal effects were observed immediately or within the first few hours post exposure. In rabbits, a large reflective spot around 200 µm to 500 µm in diameter developed over the 24 h period following exposures ~10 s or longer. The corresponding retinal threshold was ~75 J/cm^2 incident at the cornea. By 48 h, the diameter of the retinal lesion remained the same when observed with the fundus camera although it had increased in intensity, and the lesion stabilized for several weeks.

For 1356 nm, the corneal spot diameter was reduced to 0.7 mm in order to get corneal irradiance levels comparable to 1318 nm. The cornea damage threshold was 58 J/cm^2 in rabbits and 86.9 J/cm^2 in rhesus macaques. The cataract induction threshold, or lens damage threshold, was ~ 2 times the cornea damage threshold for rabbits and ~ 5 times that for rhesus. The appearance and temporal development was similar to that of 1318 nm. No retinal lesions were observed in either species for this wavelength.

In a study conducted by Berezin *et al*., they compared the ocular damage caused by exposure of chinchilla blue rabbit corneas to 1.32 µm (Nd:YAG), 1.54 µm (Glass:Yb-Er), 1.96 µm ($BaYb_2F_8$:Er), 2.09 µm (YAG-Cr-Tm:Ho), and 2.84 µm (YLF:Er) wavelengths at sub-threshold, threshold, and super-threshold (2-4 fold higher than threshold) energy levels [50]. For 1.54 µm, 1.96 µm, and 2.84 µm, the beam diameter on the cornea was controlled with a focusing lens and a diaphragm to be 2 mm. The 1.32 µm and 2.09 µm laser output had a 400 µm diameter silica optical fiber so the tip was placed very close to the cornea's surface to produce and approximately 400 µm diameter spot. Exposures at 1.32 µm lasted for 150 µs while at all other wavelengths they lasted 2 ms. Post exposure examinations consisted of a clinical evaluation, slit lamp, light microscopy, fluorescent staining, and biochemistry. The authors used probit analysis to obtain the threshold energy (ED_{50}) and radiant exposure (HD_{50}). They conclude that the calculated HD_{50}s are well correlated with the corneal absorption coefficient. The following 5 paragraphs summarize the results obtained at each of the 5 wavelengths studied.

For a wavelength of 1.32 µm, the exposures lasted for 150 µs. At 90 mJ, the authors observed grey cloudy opacities in all cornea layers, *i.e*. from the epithelium to the endothelium, with the size of the damage being approximately equal to the spot size. As the energy increased to 2 to 3 times the threshold energy, the corneal tissue at the injury site increased in optical density, *i.e*. became more opaque, but there was no damage to the iris, lens, or retina. At energies 4 times the threshold energy, there was damage to the iris as evidenced by a dark spot 400 µm to 600 µm in diameter but no iris perforation, vitreous or retinal injury. During all laser exposure, there was a noticeable forward and reverse motion of the iris. The authors found an ED_{50} of (0.11 ± 0.01) J, which corresponds to a HD_{50} of (91.6 ± 9) J/cm^2. For ease of comparison to the other exposure conditions in the study, the authors scaled the HD_{50} to a 2 mm diameter beam [51] and 0.002 s exposure duration [52]. This scaling resulted in a radiant exposure threshold of (24 ± 2) J/cm^2.

At an exposure wavelength of 1.54 µm, slight clouding of superficial cornea layers was observed at 7 J/cm^2. Subsequent increases in energy led to epithelium fluorescence staining and microscopic changes in the epithelium and anterior stroma layers. The authors obtained an HD_{50} of (7.2 ± 0.6) J/cm^2. When the exposure energy reached 13 J/cm^2, the irradiated cornea volume had a grey-white appearance, included the whole cornea thickness and was shaped as a truncated cone with the posterior base diameter smaller than the anterior base. Exposures in the 23 J/cm^2 to 30 J/cm^2 range caused cylindrical white damage along the laser's path. There was swelling around the main injury (up to 200 µm in width). As the exposure dose increased, the diameter of the anterior injury increased as well as the width of the swelling (1000 µm to 1200 µm). Around 30 J/cm^2 to 60 J/cm^2 produced excessive epithelium coagulation with initial signs of carbonization. After 1 to 2 days, necrotic tissue was observed. Higher exposure energies caused severe carbonization of the epithelium, opacity of the stroma and formation of star shaped corneal folds with local scarring

and loss of corneal sphericity. In all cases, the irritation of the anterior eye segment was light or moderate and passed in 4 to 6 days with complete restoration of the anterior epithelium and reduction of the cornea opacity. There were no clinical features of damage to the iris or lens.

For 1.96 μm, tissue changes were observed at 3 J/cm^2 to 3.5 J/cm^2 as energy increased. During exposure, opalescent dot opacities appeared in the external layers of the anterior epithelium, but were only observed for 2 h to 3 h post exposure. There was no fluorescence or marked eye irritation. As the laser irradiation increased, the coagulation of the corneal layers along the laser beam path appeared deeper. At 13 J/cm^2, an intense grey-white opacity with sharp borders was observed and the slit lamp showed that it extended 250 μm deep with no damage to the posterior cornea layers. Fluorescein showed intensive staining at the site of exposure, swelling, and partial detachment of the epithelium at the margins of the injury. There was light eye irritation for several days post exposure but full epithelization occurred in 4 to 6 days. There was no inflammatory reaction of the iris or ciliary body, and no evidence of cataract formation. Between 6 to 10 days after exposure, the intensity of the opacity diminished and after 20 to 60 days, semitransparent clouding was observed. The authors obtained an HD_{50} of (2.9 ± 0.5) J/cm^2.

At an exposure wavelength of 2.09 μm, the first signs of a coagulation effect were observed with increasing energy at an energy of 9.5 mJ, although there was no fluorescent staining. At 12.5 mJ, an area of the epithelial layer appeared grayish at the exposure site. Increasing the energy to 28 mJ led to a deeper injury extending 200 μm, but there was no biomicroscopical or histological evidence of damage to the stroma. At 35 mJ to 65 mJ, a full-thickness 400 μm in diameter coagulate was formed. In some cases, a superficial crater was formed which showed carbonization. An energy of 110 mJ led to severe coagulation, carbonization, enlargement of the crater, and the injury of the epithelium extending to a width of 500 μm. However, there was no clinical or histological evidence of damage or disturbance to the eye structures behind the cornea. Healing of the coagulated corneal areas was similar to that mentioned above. In this case, the ED_{50} was (1.1 ± 1.2) ×10^{-3} J, which corresponds to a HD_{50} of (9.3 ± 1.1) J/cm^2. For ease of comparison to the other exposure conditions in the study, the authors scaled the HD_{50} to a 2 mm diameter beam [51] which resulted in a radiant exposure threshold of (3.7 ± 0.2) J/cm^2.

Laser irradiation at 2.84 μm did not produce any observable tissue damage below 0.8 J/cm^2. However, fluences above 0.8 J/cm^2 produced epithelial damage with fluorescent staining without affecting the stroma but healed within 2 to 3 days. Increasing the fluence to 2.5 J/cm^2 resulted in the formation of a crater at the location of exposure. After healing, a semitransparent opacity remained within the epithelium layer but the stroma was intact. At 2.5 J/cm^2 to 5.5 J/cm^2, there appeared to be carbonization at the bottom of the crater and on the edges. About 100 μm of the stroma became grayish and opaque but the underlying stroma was intact. Fluorescent staining remained within the eye up to 3 days after exposure, and complete epithelization occurred within 5 to 6 days. The cloudy opacity of the external layers of the cornea diminished over time but was still observable 60 days post exposure. Increasing the fluence up to 8.5 J/cm^2 resulted in a deeper crater and an increase in the coagulated layer down to 150 μm, but the deeper stromal layers appeared transparent and unchanged. Eye irritation disappeared in 6 to 10 days at which time epithelization was complete. The transparency of the stroma gradually increased but the cloudy opacity of the external layers of the cornea was still observable 60 days post exposure. There was

no evidence of damage to any of the internal eye tissues. In this case, the HD_{50} was (0.19 ± 0.03) J/cm^2.

Jiao *et al*. determined the ED_{50} and studied ocular damage caused by a single, 5 ms long pulse at 1338 nm for various spot size diameters [53]. They obtained the *in vivo* corneal damage threshold caused by a focused laser beam in New Zealand white rabbits, and the retinal damage threshold from a collimated 5.0 mm diameter beam in chinchilla grey rabbits. The laser source was a pulsed Nd:YAG solid-state laser pumped by a Xenon lamp. The laser's irradiance was approximately a top-hat distribution verified using the knife-edge technique. For the determination of corneal damage, they utilized a 5 mm circular variable aperture and an 80 mm (at 587.6 nm) focusing lens to control the spot diameter at the cornea by adjusting the position of the cornea relative to the focal spot. They used the ablation of a graphite plate as well as the knife-edge technique to determine the spot diameters. Prior to any exposures, the authors examined the corneas using a slit lamp and the retina using a fundus camera. They examined the cornea, lens and retina with a slit lamp and a fundus camera for damage immediately, 1 h, 6 h, 24 h, and 48 h post exposure. For the 1.91 mm and 3.55 mm spot diameters, it was hard to examine the retina when there was corneal damage. Histopathology was performed 24 h post exposure. Around threshold level exposures, the lesions were distinguishable by the naked eye, but hard to photograph. They appeared 1 h post-exposure, became more distinctive 6 h post-exposure, and became less visible at 24 h. No obvious distortions were found for these lesions, which involved the full thickness of the cornea. The size of the lesions was approximately equal to the spot size. The epithelial cells were arranged in disorder, the number of cell nuclei in the stroma decreased, and there was cell proliferation in the endothelial layer. Around ~1.5 times the ED_{50}, the lesions appeared as porcelain white circular spots to the naked eye and were observed immediately after exposure. Obvious distortions were found for these lesions, their edges were distinguishable from the surrounding tissue, and they involved the full corneal thickness, see Figure 11. Notably, lenticular damage was observed directly behind the corneal lesion but no retinal damage. At 24 h post-exposure, the thickness of the corneal damage regions increased. The epithelium disappeared and the damaged area did not appear to have a homogeneous surface. The lesion/no lesion data from the 6 h examination was analyzed using a statistical package and Bliss probit analysis was used to obtain the ED_{50} thresholds, fiducial limits at 95% confidence level and slopes. They found a corneal ED_{50} (95% fiducial limits) of 70.3 (68.6, 71.9) J/cm^2 for a spot diameter of 0.28 mm, 35.6 (33.8, 36.3) J/cm^2 for a 0.94 mm diameter beam, 29.6 (28.3, 30.8) J/cm^2 for a 1.91 mm diameter beam, and 30.3 (28.8, 31.8) J/cm^2 for a 3.55 mm diameter beam. For the retinal damage determination, the authors used the collimated beam such that the beam diameter at the cornea was 5.0 mm. A fundus camera was used to observe the retina and select the sites for exposure. The rest of the study was similar to that for the cornea damage thresholds except that histopathology was performed 48 h or 72 h post exposure. In brief, they found that the 24 h retinal ED_{50} (4.60 J/cm^2) was lower than the 1 h (4.83 J/cm^2). No lens or corneal damage was observed at any energy level. The authors state that for a collimated beam with a corneal spot size smaller than the pupil diameter, the retinal damage threshold can be considered a constant value, *i.e*. it does not depend on the corneal spot size. In that case, when comparing the retinal damage threshold with the corneal damage threshold as a function of the incident corneal spot diameter, it appears that, for a 5 ms pulse at 1338 nm, when the spot diameter at the cornea is smaller than 2.0 mm the cornea would be damaged before the retina. As the spot diameter increases above 2.0 mm, then the retina has a higher risk of damage.

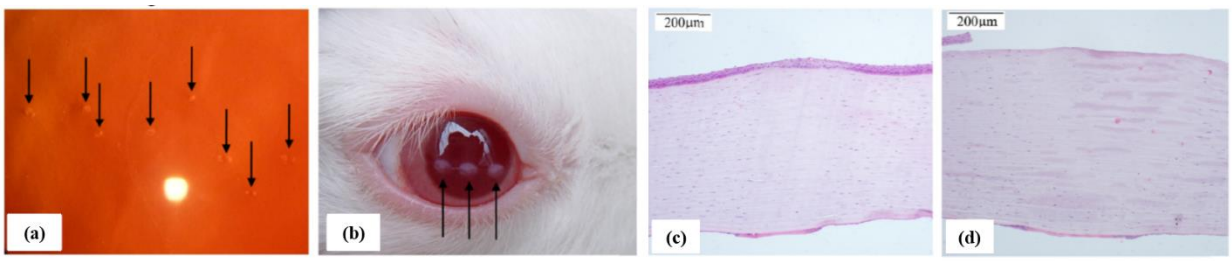

Figure 11. Corneal damage observations induced by 1338 nm pulse laser. Arrows indicate corneal lesions. (a) Lesions with a spot size of 0.28 mm at 6 h postexposure. Radiant exposure was 72.1 J/cm^2, approximately threshold level. (b) Lesions immediately after exposure. Spot size was 1.91 mm and the radiant exposure was 44.4 J/cm^2 or about 1.5 times threshold level. (c) Histological section of corneal tissue at threshold level. Same conditions as (a). Epithelium appeared disordered, the number of cell nuclei in the stroma was reduced, there was cell proliferation in the endothelium layer. (d) Histological section of corneal tissue at 1.5 times threshold level. Same conditions as (b). Epithelial layer has disappeared.

Figure 12 plots the cornea damage thresholds from the studies reviewed in Sections 4.1 and 4.2.1 with respect to exposure time and radiant exposure threshold. The skin MVL damage thresholds at 1540 nm, 1940 nm, and 2000 nm are provided as well, for reference.

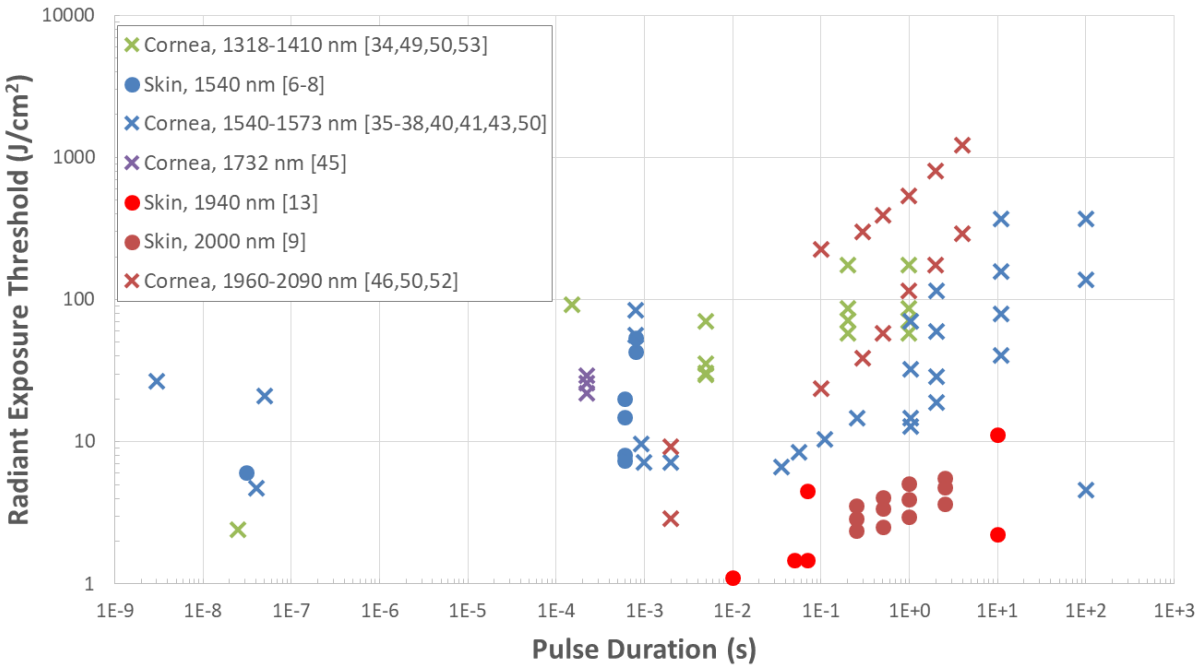

Figure 12. Cornea and skin MVL thresholds between 1318 nm and 2090 nm. Fiducial limits for these thresholds are available in the tables in Appendices A and B.

Table B.1, Table B.2, and Table B.3 contain the corneal damage thresholds from the reviewed literature. Table B.4 contains the cataract formation thresholds. The relevant laser wavelength, pulse duration, beam diameter, radiant exposure threshold, species, and literature source are listed in each table.

4.2.2. Ablation threshold determination

The next section briefly discusses the ablation threshold of cornea using UV wavelengths before covering reports on the ablation threshold of cornea at 800 nm [54], 1025 nm [30], 1053 nm [55-57]. In the following, note that there are several different criteria and associated procedures to determine the ablation threshold. Several of the studies at mid-infrared wavelengths are focused on nanosecond-to-femtosecond laser pulse durations in order to better understand the pulse duration dependence. There are two reports solely focused on pulse durations < 100 fs [58, 59] which we will omit, and will not include reports on laser-induced cavitation damage.

Laser vision correction (LVC) using UV excimer lasers was developed in the late 1980's and is based on the process of photoablation. Current procedures, such as photorefractive keratectomy (PRK) and Laser Assisted In Situ Keratomileusis (LASIK), utilize photoablation to reshape the cornea. The study by Krauss *et al*. includes a summary of the early studies on corneal response to UV light as well as the characteristics of excimer tissue ablation [60]. A more recent discussion on the interactions of excimer lasers with the cornea was presented earlier this year by Vinciguerra *et al*. [61]. However, most of the literature in that topic is primarily concerned with fluence levels as related to corneal etch rate and not ablation thresholds *per se*.

In 2007, Giguere *et al*. conducted a study to elucidate how the surface ablation threshold of silica, porcine cornea epithelium and stroma depend on the laser pulse duration (100 fs to 5 ps) for a wavelength of 800 nm [54]. In this study, the authors define the ablation threshold as "the minimum energy per unit surface (fluence) required to induce detectable changes in a material." The laser used was an amplified Ti:Sapphire laser with a continuously variable pulse duration of 100 fs to 5 ps and a 10 Hz repetition rate. However, exposures were for single shots. A half wave-plate and a polarizer were used to control the laser energy delivered. The beam was focused on the sample's surface with a microscope objective such that the average focal spot diameter was 8 μm (defined at $1/e^2$ intensity points). The sample was mounted on an XYZ translation stage and typical experiments involved ~50 exposure sites. After exposure, an optical microscope in 20x reflection mode was used to examine and measure the visible damage area for each laser shot. The ablation appeared as small shallow holes or craters. Fresh porcine eyes were obtained from a slaughterhouse and preserved at 4°C for, at most, 8 h after death. Corneal layers were prepared and laid flat on a glass slide prior to exposure. For measurements on the stroma, the epithelium was removed with a surgical blade prior to exposure. Samples were examined immediately after exposures. The authors defined the ablation threshold as the maximum fluence for which they could not observe a crater. Using this definition and 3 measurements for each pulse duration, they obtained the following ablation thresholds for the corneal epithelium: 1.24 J/cm^2 for 100 fs pulse duration, 1.41 J/cm^2 for 300 fs, 1.57 J/cm^2 for 500 fs, 1.68 J/cm^2 for 800 fs, 1.94 J/cm^2 for 1 ps, 2.38 J/cm^2 for 2 ps, 2.98 J/cm^2 for 3 ps, and 3.52 J/cm^2 for 5 ps. The nominal uncertainty associated with these ablation thresholds was between 14.4 and 17.3%. For the corneal stroma, the authors reported the following ablation thresholds: 1.51 J/cm^2 for 100 fs pulse duration, 1.60 J/cm^2 for 300 fs, 1.89 J/cm^2 for 500 fs, 1.96 J/cm^2 for 800 fs, 2.27 J/cm^2 for 1 ps, 2.50 J/cm^2 for 2 ps, 3.13 J/cm^2 for 3 ps, and 4.77 J/cm^2 for 5 ps. The nominal uncertainty associated with the corneal stroma ablation thresholds was between 14.8 and 15.3%. Note that the data was extracted from a graph. The uncertainties were calculated from the error bars associated with the data in the graph. The authors also presented a model which includes the physical mechanisms related to laser-induced damage

which shows good agreement with the data. From the data, they conclude that the ablation threshold showed a plateau-like region between 100 fs and ~1 ps, and it increased for larger pulse durations. In a follow up study, the authors studied the wavelength dependence of the ablation threshold for 100 fs long pulses between 800 nm and 1450 nm [58]. The main finding from that study is that the ablation threshold varied only slightly between 1.5 J/cm^2 and 2.2 J/cm^2 within that wavelength range.

In the study conducted by Hoffart *et al*., the authors described a characterization technique to measure laser damage of corneal tissues, *i.e*. the epithelium and Bowman's membrane [30]. They utilized a commercial s-pulse device delivering 450 fs long pulses at a wavelength of 1025 nm at a 1 kHz repetition rate to irradiate human corneas not suitable for transplant. The beam was enlarged to a diameter of 8 mm at the $1/e^2$ intensity points, before being focused on the sample with a 100 mm focal length plano-convex lens. The laser intensity distribution is Gaussian and the focal spot size was measured as 10.7 µm while the Rayleigh range was 350 µm. The fluence was calculated using a top-hat equivalent surface, *i.e*. a uniform cylindrical beam with a smaller radius but the same energy and peak fluence as described in [62]. A far-field imaging system was also incorporated into the set up to visualize the surface of the cornea, which is translated to a new location for each test. Eyes were obtained from an organ donation site within 36 hours of death and were stored in a solution for less than 10 days. The cornea was removed from the rest of the eyeball prior to exposures. In order to ablate the Bowman's membrane, a surgical sponge was used to remove the epithelium prior to exposures. The corneas were placed on an artificial anterior chamber of the Barron type. Saline was injected in order to inflate and pressurize the cornea from its posterior surface. Typically, a 1 mm^2 area was used for exposures at a range of fluences and up to 100 shots were located within that area. Ten exposures at the same fluence level were performed before varying the fluence and repeating this procedure. The sample was then examined with an optical microscope to score the exposed sites (0/1 = no-damage/damage). Damage was defined as an irreversible and permanent modification of the surface examined at high magnification. This enabled the determination of two values: the maximum fluence for which damage was always absent ($F_{th,\,low}$), *i.e*. the highest fluence with a score of 0, and the minimal fluence for which damage was always detected ($F_{th,\,high}$), *i.e*. the lowest fluence with a score of 1. From these experiments the authors determined the thresholds of damage for the epithelial layer to be $F_{th,\,low} = 2.7 \pm 0.1$ J/cm^2 and $F_{th,\,high} = 5.6 \pm 0.4$ J/cm^2, which are significantly lower than those for the Bowman's layer $F_{th,\,low} = 3.4 \pm 0.1$ J/cm^2 and $F_{th,\,high} = 7.1 \pm 1.1$ J/cm^2. These number are averages over three different samples. The damage determinations for the epithelium are less reproducible and have more fluctuations than for the Bowman's layer. The authors noted that near the corneal tissue threshold for ablation, there was a large variation in the morphology of the damaged area, even for a constant fluence. As shown in Figure 13, some craters were hardly visible and the diameters could not be measured with precision. At higher fluences, the damage became more reproducible, however, the shapes were not regular so determining a diameter was still challenging.

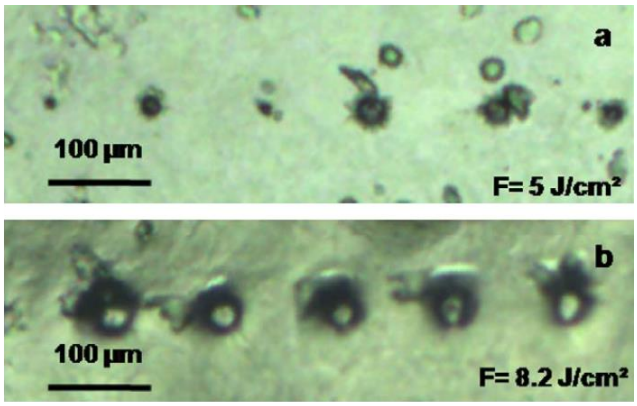

(a)

(b)

Figure 13. Photographs of damage to the epithelium obtained for 1025 nm at two different fluences (a) close to the threshold of damage and (b) about 1.6 times the threshold for damage.

Loesel *et al*. used human corneas, human enamel, and bovine brain tissue to determine the laser-induced optical breakdown (LIOB) of those materials as a function of pulse duration [55]. They utilized a multistage dye laser system capable of generating amplified pulses at a wavelength of 630 nm, 1 kHz repetition rate and continuously variable pulse duration between 80 fs and 10 ps. In addition, they utilized an Nd:YAG laser system to generate pulses at a wavelength of 1053 nm with pulse durations varying between 30 ps and 200 ps at a 1 kHz repetition rate. The eyes were enucleated several hours prior to the experiments but were kept chilled until the beginning of the experiments. The laser beams were both focused onto the cornea with a microscope objective such that the focal spot diameter was ~ 5 µm as measured using the knife edge technique. During the experiments, the energy of the laser was continuously decreased from above threshold values while scattered light from a CW probe beam was monitored. In addition, the surface of the tissue was observed with a high resolution optical microscope. When cavitation bubbles and material removal occur, the probe beam was scattered. When no cavitation bubbles or ejected material were produced, the intensity of the scattered light decreased dramatically. This event coincides with the disappearance of tissue damage observed with the optical microscope, therefore, the ablation damage threshold was defined by the drop in intensity of the scattered light. The authors report the fluence at threshold for single-pulse energies, which are obtained from the average output power of the 1 kHz pulse trains. Data represent mean values averaged over 3 to 5 samples. For human corneas, the LIOB threshold for 630 nm was 1.98 J/cm^2 for 350 fs pulse duration, 2.57 J/cm^2 for ~960 fs, 3.17 J/cm^2 for 2 ps, 5.28 J/cm^2 for ~6 ps, and 8.79 J/cm^2 for ~10 ps. For 1053 nm, the LIOB thresholds were 20 J/cm^2 for ~30 ps, 26 J/cm^2 for ~60 ps, and 40 J/cm^2 for 200 ps. The data listed were extracted from a graph. According to the authors, the nominal uncertainty associated with the determination of the LIOB thresholds is dominated by the uncertainty is determining the focal spot size (±15%). Notably, the LIOB threshold decreased as the pulse duration decreased. The authors also presented a model to describe the dependence of LIOB threshold fluence on the pulse duration, which shows good agreement with their data and predicts a square root behavior on pulse duration.

In another study, Sun *et al*. determined the threshold radiant exposure for breakdown by monitoring the laser-induced plasma and the second harmonic generation (SHG) signal from the cornea's collagen at various pulse durations ranging from 800 fs to 20 ps [56]. For these experiments, they performed single shot exposures and utilized three different diode pumped all-

solid-state ultrafast lasers delivered through identical delivery systems in order to keep the ablation conditions the same. The Nd:glass femtosecond laser emitted pulses at 1053 nm where the pulses can be continuously varied from 800 fs to 5 ps pulse durations at 76 MHz repetition rate. The Yb:KYW femtosecond laser is a thin disk regenerative amplifier that produces 800 fs long pulses with a bandwidth spanning from 1000 nm to 1060 nm. The Nd:YAG emits 20 ps long pulses at 1064 nm. The laser intensity from the 3 sources was varied using a half wave-plate and linear polarizer combination. A beam expander was used to overfill the back of a 5x, 0.12 NA microscope objective. The objective served to focus the laser beam inside the sample and to collect the plasma spark generated. The knife edge technique was used to determine the focal spot sizes. A second 20x objective, 0.4 NA was placed after the sample to collect the SHG signal. Excised porcine eyeballs were obtained from a slaughterhouse and used within 12 hours. Before the experiment, the epithelium was carefully removed in order to eliminate any confounding effects due to post-mortem changes in the epithelium. During the experiments, the authors monitored the light emitted during plasma formation as well as the SHG signal. When the laser irradiates the cornea, it generates a plasma due to laser induced optical breakdown. When the tissue is ablated, it loses its ability for SHG, therefore the SHG signal decreases as the plasma increases. The threshold of the corneal stromal ablation was determined by the combined decrease in SHG and increase in the plasma spark. The authors ablated the same cornea with the different laser and pulse durations and found the following ablation thresholds: 4.8 J/cm^2 for 20 ps, 1.69 J/cm^2 for 2.86 ps, 1.19 J/cm^2 for 1.6 ps, and 0.6 J/cm^2 for 800 fs. In addition, the authors studied the intrastromal ablation threshold at various depths inside the stroma. They did not find a significant dependence of the cornea ablation threshold on the depth into the stroma down to a depth of 200 µm. The authors conclude that the ablation threshold is proportional to the square root of the laser pulse duration for the data above 2 ps and that multi-photon effects start to dominate for shorter pulse durations.

Oravesky *et al*. also studied plasma mediated ablation at 1053 nm for pulse durations between 1 ns and 300 fs in excised porcine corneas and collagen gels [57]. They utilized a Ti:sapphire chirped pulse amplifier (CPA) system, which produced Gaussian pulses at a repetition rate of 10 Hz with continuously adjustable pulse durations from 0.3 ns to 1 ns (full width at half-maximum intensity). Single pulses were extracted for experiments. The energy delivered to the sample was adjusted with a half-waveplate before compression, using the strong dependence of grating efficieny upon input polarization. The laser spot diameter used for ablation was 0.5 mm (full width at 1/*e* of intensity) where the laser was focused onto the sample with a 1 m focal length lens such that the distance to the sample could be varied. The spot size was measured with a CCD camera and the laser spatial mode showed a 98% fit to a Gaussian. Fresh porcine eyes were obtained from a slaughterhouse, preserved on ice and used within 2 h. Collagen gels were prepared from gelatin with other components (cupric sulfate, polystyrene beads, carbon black micro-powder) in order to control the absorption coefficient from ~ 0.1 cm^{-1} to 1000 cm^{-1}. Thin slabs (25 × 25 × 1.85) mm were cut for the experiments. Eyeballs were held in a custom-made holder so the front surface of the cornea could be exposed. After irradiation, the sample was examined with a Nomarski microscope (differential interference contrast microscopy). The ablation threshold was defined as any visible permanent removal of material from the surface as visualized with the Nomarski microscope. Therefore the ablation threshold fluence was the fluence at which a minimal visible crater on the surface was produced by 10 laser pulses at a 1 Hz repetition rate. The smallest craters observed were approximately 1 µm in diameter. The authors also used optical microscopy to examine the topography of the craters. The Nomarski microscope was equipped with a micron grid

to aid in measuring the diameter of the craters, while the crater depth was measured by focusing the microscope to the top surface and then the bottom surface of the crater using a calibrated micro-screw. The ablation thresholds for cornea (clear collagen gel without cupric sulfate) were approximately 0.28 (0.26) J/cm^2 for 350 fs, 7 (5) J/cm^2 for 20 ps, 25 (17) J/cm^2 for 150 ps, and 64 (46) J/cm^2 for 900 ps. For the collagen gel with cupric sulfate (with carbon black micropowder), the ablation thresholds found were 0.22 (0.07) J/cm^2 for 350 fs, 1.4 (0.09) J/cm^2 for 20 ps, and 6.5 (0.1) J/cm^2 for 900 ps. The authors concluded that the threshold laser fluence for ablation of cornea depends on the pulse duration and is very similar to that of clear collagen gels. However, in the femtosecond range, the threshold laser fluence for ablation of cornea approaches the value for collagen gels with carbon black micropowder. Similarly to the studies by Sun *et al*. [56] and Loesel *et al*. [55], the authors observed similar square root dependence on the pulse duration, with a possible deviation in the femtosecond range. They also characterized the crater drilling rate in the clear collagen gel for the 350 fs pulse duration as a function of laser fluence. The craters produced in the clear collagen gel with 350 fs long pulses had clean edges and were smooth as opposed to the ones created with nanosecond pulses, which were irregularly shaped craters. In addition, the authors discuss the origin of the differences in the crater's appearance and attribute them to the physical mechanism responsible for energy deposition; multiphoton ionization for femtosecond and sub-picosecond pulses and linear absorption for sub-nanosecond and nanosecond pulses.

Table C.1 and Table C.2 contain the corneal ablation radiant exposure thresholds for the reviewed literature, and includes laser wavelength, pulse duration, beam diameter, sample type, and source for each threshold. A plot of the corneal ablation thresholds is provided in Figure 14.

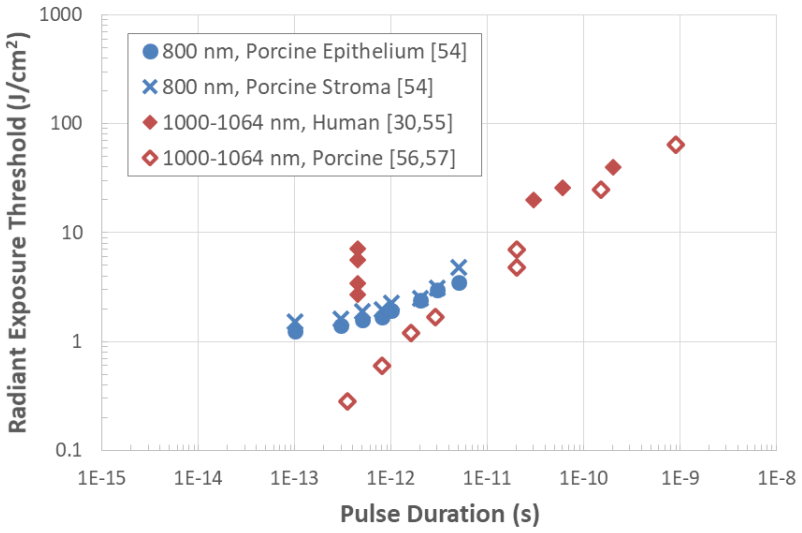

Figure 14. Corneal ablation thresholds. Fiducial limits for these thresholds are available in the tables in Appendix C.

5.0 CONCLUSION

This document provides a robust overview of threshold-level laser-induced damage to skin and cornea in the 1400 nm to 2000 nm wavelength range. Furthermore, we have provided a review pertaining to supra-threshold laser-induced damage to skin and cornea, though these are not necessarily limited to the 1400 nm to 2000 nm wavelength range given limitations of data.

Skin MVL threshold data points in this particular wavelength region are limited to a few studies, particularly at 1540 nm, 1940 nm, and 2000 nm. The majority of these data points are for continuous-wave or switched continuous-wave laser systems where the damage mechanism is primarily thermal. These studied wavelengths feature relatively high water absorption compared to visible and near-infrared regions, and thus rapid accumulation of heat at the surface of the skin.

Supra-threshold laser exposure to skin is common in certain medical applications such as surgical cutting, but these circumstances are quite unique and not feasible in the context of dose response modeling. Perhaps the most useful approach to supra-threshold laser-induced damage to skin would be determination of dose requirements for particular burn degrees and dermal penetration. However, at this point, such studies have not been performed. Among the most relevant skin supra-threshold studies are the investigation by Fan *et al*. [21] that correlated wound healing across a 28 day time period with laser dose, and the work done by DeLisi *et al*. [23] on steam blister formation in excised porcine skin. These studies utilized a near-infrared wavelength of 1064 and 1070 nm, respectively, which penetrates deep into skin, unlike those between 1400 and 2000 nm.

One of the goals of this literature review was to identify ways to measure severity of outcome to corneal tissue from exposures to laser light between 1400 and 2000 nm. In order to do so, we surveyed around 32 publications and were able to roughly categorize the damage reported into 3 main groups. Minimum visible lesions (MVL) are threshold lesions that appear within 1 h from exposure and are identified as such using a slit lamp. They are associated with the radiant exposure damage thresholds used to establish laser safety standards. As the radiant exposure increases above threshold, larger diameter lesions, which involve multiple layers and are visible immediately after exposure have been documented. Under certain conditions, damage can involve multiple ocular components, such as the cornea, lens, and/or retina. These lesions may or may not cause long term damage and are in a sub-ablative regime, so we are proposing to identify them as first degree supra-threshold lesions as depicted in Figure 15.

As the radiant exposure increases, there can be permanent removal of material, i.e. ablation, and carbonization for exposure durations in the millisecond range. We are proposing to identify these lesions as second degree supra-threshold lesions. However, it should be pointed out that corneal lesion identification in this wavelength regime is based on subjective criteria to describe the appearance of the lesions. In addition, there is a large variability in the experimental conditions used for damage threshold determinations and in both, the experimental conditions and definitions for ablation threshold determinations, making comparisons between the results reported difficult. It should be noted that studies to determine damage thresholds are primarily *in vivo*, while ablation threshold studies are in excised tissue. It is also important to note that appearance, size, and depth of the lesions and amount of time they take to heal, strongly depends on the wavelength, laser energy, beam diameter, and pulse duration.

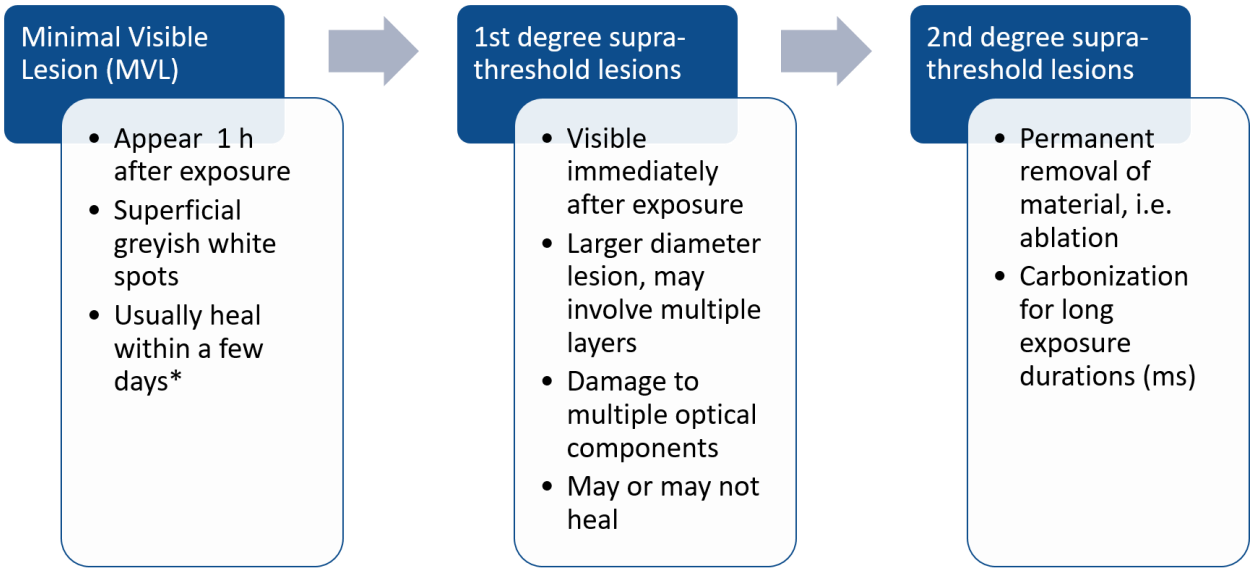

Figure 15. Proposed classification of corneal injuries.

Currently, published cornea damage thresholds in the 1400 nm to 2000 nm wavelength range are limited to only 7 wavelengths: 1410 nm, 1540 nm, 1550 nm, 1573 nm, 1732 nm, 1960 nm, and 2000 nm. Given that the absorption coefficient of water changes rapidly in the 1850 nm to 1950 nm regime, obtaining damage thresholds in this region would help inform the laser safety standards community. In addition, there are no published cornea damage thresholds for pulses longer than 50 ns or pulses shorter than hundreds of µs at those wavelengths. Obtaining cornea damage thresholds for the pulse durations that are missing, would be very informative for the laser safety community. At wavelengths of 1318 nm, 1320 nm, 1338 nm, and 1356 nm, there are reports of damage involving multiple ocular components, including cataract formation in the lens, and/or damage to the iris and/or retina. Pulse durations were 150 µs for 1320 nm and between 0.2 s and 1 s for 1318 nm, 1338 nm, and 1356 nm. In terms of ablation thresholds, there are no data within the 1400 nm to 2000 nm regime. Addressing this data gap by obtaining ablation thresholds at any of these wavelengths would be very informative. In this technical note we have included reports of ablation thresholds at 800 nm, 1000 nm to 1060 nm, 1025 nm, 1053 nm, and 1064 nm although those reports were obtained for pulse durations in the ultrashort regime (between 100 fs and 1 ps).

Several of the studies reviewed here note that the ablation threshold is proportional to the square root of the laser pulse duration for pulse durations longer than ~2 ps, where laser induced optical breakdown in responsible for the removal of material. Multi-photon effects are expected to dominate the ablation process for pulse durations shorter than ~100 fs. Confirmation if this square-root relationship on pulse duration holds for wavelengths longer than 1400 nm is crucial for updating and enhancing current dose response models.

6.0 REFERENCES

[1] E. M. Ahmed, E. A. Early, D. F. Huantes, D. A. Wooddell, and R. J. Thomas, "A Probabilistic 1064 nm Dose Response Model, Version 1.0," Air Force Research Laboratory, Ft. Sam Houston, TX AFRL-RH-BR-TR-2009-0021, 2009.

[2] E. M. Ahmed, E. A. Early, P. Kennedy, and R. J. Thomas, "Human Laser Retinal Dose-Response Model," Air Force Research Laboratory, Ft. Sam Houston, TX, Tech Report No. AFRL-RH-FS-TR-2018-0006, 2018.

[3] E. M. Ahmed, E. A. Early, P. Kennedy, and R. J. Thomas, "Human Variability in Laser Retinal Dose-Response Modeling," Air Force Research Laboratory, Ft. Sam Houston, TX AFRL-RH-FS-TR-2018-0007, 2018.

[4] E. M. Ahmed, E. A. Early, B. J. Lund, and R. J. Thomas, "Human Laser Skin Dose-Response Model," Air Force Research Laboratory, Ft. Sam Houston, TX AFRL-RH-FS-TR-2020-0018, 2020.

[5] T. A. Eggleston, W. P. Roach, M. A. Mitchell, K. Smith, D. Oler, and T. E. Johnson, "Comparison of two porcine (Sus scrofa domestica) skin models for in vivo near-infrared laser exposure," *Comparative Medicine,* vol. 50, pp. 391-397, 2000.

[6] C. P. Cain, K. J. Schuster, J. J. Zohner, K. L. Stockton, D. J. Stolarski, R. J. Thomas, B. A. Rockwell, and W. P. Roach, "Visible lesion thresholds with pulse duration, spot size dependency, and model predictions for 1.54-μm, near-infrared laser pulses penetrating porcine skin," *Journal of Biomedical Optics,* vol. 11, p. 024001, 2006.

[7] P. J. Rico, T. E. Johnson, M. A. Mitchell, B. H. Saladino, and W. Roach, "Median effective dose determination and histologic characterization of porcine (Sus scrofa domestica) dermal lesions induced by 1540-nm laser radiation pulses," *Comparative Medicine,* vol. 50, pp. 633-638, 2000.

[8] W. P. Roach, J. J. Thomas, K. J. Schuster, K. Stockton, D. J. Stolarski, M. S. Foltz, B. A. Rockwell, and C. P. Cain, "Model predictions and measured skin damage thresholds for 1.54-μm laser pulses in porcine skin," *Proc. SPIE,* vol. 4961, pp. 90-97, 2003.

[9] B. Chen, D. C. O'dell, S. L. Thomsen, B. A. Rockwell, and A. J. Welch, "Porcine skin ED50 damage thresholds for 2,000 nm laser irradiation," *Lasers in Surgery and Medicine,* vol. 37, pp. 373-381, 2005.

[10] B. Chen, D. C. O'dell, S. L. Thomsen, R. J. Thomas, and A. J. Welch, "Effect of Pigmentation Density upon 2.0 μm Laser Irradiation Thermal Response," *Health Physics,* vol. 93, pp. 273-278, 2007.

[11] B. Chen, S. L. Thomsen, R. J. Thomas, and A. J. Welch, "Modeling thermal damage in skin from 2000-nm laser irradiation," *Journal of Biomedical Optics,* vol. 11, p. 064028, 2006.

[12] B. Chen, S. L. Thomsen, R. J. Thomas, J. Oliver, and A. J. Welch, "Histological and modeling study of skin thermal injury to 2.0 μm laser irradiation," *Lasers in Surgery and Medicine,* vol. 40, pp. 358-370, 2008.

[13] J. W. Oliver, D. J. Stolarski, S. S. Kumru, C. P. Cain, C. J. Finkeldei, I. D. Noojin, R. J. Thomas, G. D. Buffington, G. D. Noojin, and H. M. Hodnett, "Infrared skin damage thresholds from 1940-nm continuous-wave laser exposures," *Journal of Biomedical Optics,* vol. 15, p. 065008, 2010.

[14] M. P. DeLisi, K. J. Schuster, G. D. Noojin, A. J. Tijerina, A. D. Shingledecker, M. S. Schmidt, S. S. Kumru, and B. A. Rockwell, "Porcine skin damage thresholds for multiple-pulse laser exposure at 1940 nm," *Proc. SPIE,* vol. 11238, p. 112380C, 2020.

[15] M. P. DeLisi, G. D. Noojin, A. M. Peterson, A. J. Tijerina, A. D. Shingledecker, M. S. Schmidt, K. J. Schuster, S. S. Kumru, and B. A. Rockwell, "Investigation of Multiple-Pulse Mid-Infrared Laser Skin Damage Thresholds in the Yucatan Mini Pig," Air Force Research Laboratory, Ft. Sam Houston, TX2020.

[16] A. I. Metelitsa and T. S. Alster, "Fractionated laser skin resurfacing treatment complications: a review," *Dermatologic Surgery,* vol. 36, pp. 299-306, 2010.
[17] D. K. Hysell and A. S. Brownell, "Correlation between the gross and microscopic appearance of CO2 laser induced porcine skin burns," Army Medical Research Laboratory, Ft Knox, KY AD0676578, 1968.
[18] N. Museux, L. Perez, L. Autrique, and D. Agay, "Skin burns after laser exposure: Histological analysis and predictive simulation," *Burns,* vol. 38, pp. 658-667, 2012.
[19] Y.-M. Zhang, J. Ruan, R. Xiao, Q. Zhang, and Y.-S. Huang, "Comparative study of 1,064-nm laser-induced skin burn and thermal skin burn," *Cell Biochemistry and Biophysics,* vol. 67, pp. 1005-1014, 2013.
[20] C. J. Schaffer, L. Reinisch, S. L. Polis, G. P. Stricklin, and L. B. Nanney, "Comparisons of wound healing among excisional, laser-created, and standard thermal burns in porcine wounds of equal depth," *Wound repair and regeneration,* vol. 5, pp. 52-61, 1997.
[21] Y. Fan, Q. Ma, J. Liang, Y. Lu, B. Ni, Z. Luo, Y. Cui, and H. Kang, "Quantitative and qualitative evaluation of recovery process of a 1064 nm laser on laser-induced skin injury: in vivo experimental research," *Laser Physics Letters,* vol. 16, p. 115604, 2019.
[22] Y. Fan, Q. Ma, S. Xin, R. Peng, and H. Kang, "Quantitative and Qualitative Evaluation of Supercontinuum Laser-Induced Cutaneous Thermal Injuries and Their Repair With OCT Images," *Lasers in Surgery and Medicine,* vol. 53, pp. 252-262, 2021.
[23] M. P. DeLisi, A. M. Peterson, L. A. Lile, G. D. Noojin, A. D. Shingledecker, D. J. Stolarski, C. A. Oian, S. S. Kumru, and R. J. Thomas, "Suprathreshold laser injuries in excised porcine skin for millisecond exposures at 1070 nm," *Journal of Biomedical Optics,* vol. 23, p. 125001, 2018.
[24] R. Vincelette, G. D. Noojin, C. A. Harbert, K. J. Schuster, A. D. Shingledecker, D. J. Stolarski, S. S. Kumru, and J. W. Oliver, "Porcine skin damage thresholds for 0.6 to 9.5 cm beam diameters from 1070-nm continuous-wave infrared laser radiation," *Journal of Biomedical Optics,* vol. 19, p. 035007, 2014.
[25] J. E. Tintinalli, J. S. Stapczynski, O. J. Ma, D. Cline, G. D. Meckler, and D. M. Yealy, *Tintinalli's emergency medicine: a comprehensive study guide*: McGraw-Hill Education New York, 2016.
[26] A. L. Gibson, B. C. Carney, L. Cuttle, C. J. Andrews, C. J. Kowalczewski, A. Liu, H. M. Powell, R. Stone, D. M. Supp, and A. J. Singer, "Coming to consensus: what defines deep partial thickness burn injuries in porcine models?," *Journal of Burn Care & Research,* vol. 42, pp. 98-109, 2021.
[27] M. P. DeLisi, N. J. Gamez, C. D. ClarkIII, S. S. Kumru, B. A. Rockwell, and R. J. Thomas, "Computational modeling and damage threshold prediction of continuous-wave and multiple-pulse porcine skin laser exposures at 1070 nm," *Journal of Laser Applications,* vol. 33, p. 022023, 2021.
[28] C.-y. Lyu and R.-j. Zhan, "Accurate analysis of limiting human dose of non-lethal laser weapons," *Defence Technology,* 2021.
[29] R. McCally, C. Bargeron, J. Bonney-Ray, and W. Green, "Laser eye safety research at APL," *undefined,* 2005 2005.
[30] L. Hoffart, O. Utéza, N. Sanner, F. Matonti, M. Sentis, B. Ridings, and J. Conrath, "Nouvelle approche de détermination du seuil d'endommagement de tissus biologiques par laser femtoseconde : intérêt et application à la chirurgie de la cornée," */data/revues/01815512/v33i9/S0181551210002743/,* 2010/11/23/ 2010.
[31] K. Schulmeister, D. H. Sliney, J. Mellerio, D. J. Lund, B. E. Stuck, and J. A. Zuclich, "Review of exposure limits and experimental data for corneal and lenticular damage from short pulsed UV and IR laser radiation," *Journal of Laser Applications,* vol. 20, pp. 98-105, 2008/04/22/ 2008.
[32] M. Jean, K. Schulmeister, D. J. Lund, and B. E. Stuck, "Laser-induced corneal injury: validation of a computer model to predict thresholds," *Biomedical Optics Express,* vol. 12, p. 336, 2021/01/01/ 2021.
[33] B. E. Stuck, D. J. Lund, and E. S. Beatrice, "Ocular Effects Of Laser Radiation From 1.06 to 2.06Âμ," in *Ocular Effects of Non-Ionizing Radiation*, 1980, pp. 115-120.

[34] C. J. Archibald and J. Taboada, "Damage to the cornea induced by 1.4 micrometer laser light pulses," *Annual Scientific Meeting, Aerospace Medical Association*, 1981 1981.
[35] D. J. Lund, M. B. Landers, G. H. Bresnick, J. O. Powell, J. E. Chester, and C. Carver, "Ocular Hazards of the Q-Switched Erbium Laser," *Investigative Ophthalmology & Visual Science*, vol. 9, pp. 463-470, 1970/06/01/ 1970.
[36] P. S. Avdeev, Y. D. Berezin, Y. P. Gudakovskiĭ, V. R. Muratov, A. G. Murzin, and V. A. Fromzel, "Experimental determination of maximum permissible exposure to laser radiation of 1.54 μ wavelength," *Soviet Journal of Quantum Electronics*, vol. 8, p. 137, 1978/01/31/ 1978.
[37] B. E. Stuck, D. J. Lund, and E. S. Beatrice, "Ocular Effects of Holmium (2.06 μM) and Erbium (1.54 μM) Laser Radiation," *Health Physics*, vol. 40, p. 835, 1981/06// 1981.
[38] T. E. Johnson, M. A. Mitchell, P. J. Rico, D. J. F. D.v.m, T. E. Eurell, and W. P. Roach, "Corneal and skin laser exposures from 1540-nm laser pulses," in *Laser-Tissue Interaction XI: Photochemical, Photothermal, and Photomechanical*, 2000, pp. 222-229.
[39] T. F. Clarke, T. E. Johnson, M. B. Burton, B. Ketzenberger, and W. P. Roach, "Corneal injury threshold in rabbits for the 1540 nm infrared laser," *Aviation, Space, and Environmental Medicine*, vol. 73, pp. 787-790, 2002/08// 2002.
[40] R. L. McCally, J. Bonney-Ray, and C. B. Bargeron, "Corneal epithelial injury thresholds for exposures to 1.54-um radiation," in *Laser and Noncoherent Light Ocular Effects: Epidemiology, Prevention, and Treatment III*, 2003, pp. 107-112.
[41] R. L. McCally, J. Bonney-Ray, and C. B. Bargeron, "corneal epithelial injury thresholds for exposures to 1.54 microm radiation-dependence on beam diameter," *Health Physics*, vol. 87, pp. 615-624, 2004/12// 2004.
[42] R. L. McCally and J. Bonney-Ray, "Corneal epithelial injury thresholds for multiple-pulse exposures to erbium fiber laser radiation at 1.54 μm," in *Ophthalmic Technologies XV*, 2005, pp. 423-428.
[43] W. T. Ham and H. A. Mueller, "ANSI Z136.2 Update: Ocular Effects of Laser Infrared Radiation," *Journal of Laser Applications*, vol. 3, pp. 19-21, 1991/10// 1991.
[44] D. Courant, C. Chapel, C. Billy, N. Salès, J.-C. Pérot, and C. Pothier, "In vivo and in vitro evaluation of the corneal damage induced by 1573 nm laser radiation," *Journal of Laser Applications*, vol. 20, pp. 69-75, 2008/04/22/ 2008.
[45] B. E. Stuck, D. J. Lund, and E. S. Beatrice, "Ocular effects of relatively “eyesafe” lasers," in *Conference on Combat Ocular Problems*, 1982, pp. 1-14.
[46] B. Chen, J. Oliver, S. Dutta, G. H. Rylander Iii, S. L. Thomsen, and A. J. Welch, "Corneal minimal visible lesion thresholds for 2.0 μm laser radiation," *Journal of the Optical Society of America A*, vol. 24, p. 3080, 2007/10/01/ 2007.
[47] J. A. Zuclich, D. J. Lund, B. E. Stuck, and P. R. Edsall, "Wavelength dependence of ocular damage thresholds in the near-IR to far-IR transition region (Proposed revisions to MPEs)," in *International Laser Safety Conference*, 2005, pp. 58-66.
[48] W. P. Roach, T. E. Eurell, and T. E. Johnson, "Corneal exposures from 1540-nm laser pulses," in *Laser and Noncoherent Light Ocular Effects: Epidemiology, Prevention, and Treatment*, 2001, pp. 89-96.
[49] J. Zuclich, D. Gagliano, F. Cheney, B. Stuck, H. Zwick, P. Edsall, and D. Lund, *Ocular Effects of Penetrating Ir Laser Wavelengths* vol. 2391. Bellingham: Spie - Int Soc Optical Engineering, 1995.
[50] Y. D. Berezin, E. V. Boiko, V. V. Volkov, V. F. Danilichev, D. V. Ganin, A. F. Gatzu, N. N. Smirnov, V. V. Lazo, and A. M. Tkachuk, "Peculiarities of coagulation action of IR lasers (1-3 um) radiation on cornea," in *Laser Optics '95*, 1996, pp. 9-13.
[51] V. R. Muratov, Y. D. Berezin, and Y. P. Gudakovskii, "Normalization of laser radiation," *Kvantovaya Elektron. (Moscow); (USSR)*, vol. 7, 1980/08/01/T04:00:00Z 1980.

[52] P. S. Avdeev, I. D. Berezin, V. V. Volkov, I. P. Gudakovskiĭ, and O. V. Konovalov, "[Biological action of infrared laser radiation (1.06-micron wave length) on the tissues of the fundus oculi]," *Vestnik Oftalmologii*, pp. 26-31, 1982/02//Jan- undefined 1982.

[53] L. Jiao, J. Wang, X. Jing, H. Chen, and Z. Yang, "Ocular damage effects from 1338-nm pulsed laser radiation in a rabbit eye model," *Biomedical Optics Express*, vol. 8, p. 2745, 2017/05/01/ 2017.

[54] D. Giguere, G. Olivie, F. Vidal, S. Toetsch, G. Girard, T. Ozaki, J.-C. Kieffer, O. Nada, and I. Brunette, "Laser ablation threshold dependence on pulse duration for fused silica and corneal tissues: experiments and modeling," *Journal of the Optical Society of America a-Optics Image Science and Vision*, vol. 24, pp. 1562-1568, 2007/06// 2007.

[55] F. H. Loesel, M. H. Niemz, J. F. Bille, and T. Juhasz, "Laser-induced optical breakdown on hard and soft tissues and its dependence on the pulse duration: experiment and model," *IEEE Journal of Quantum Electronics*, vol. 32, pp. 1717-1722, 1996/10// 1996.

[56] H. Sun, M. Han, M. H. Niemz, and J. F. Bille, "Femtosecond laser corneal ablation threshold: dependence on tissue depth and laser pulse width," *Lasers in Surgery and Medicine*, vol. 39, pp. 654-658, 2007/09// 2007.

[57] A. A. Oraevsky, L. B. DaSilva, A. M. Rubenchik, M. D. Feit, M. E. Glinsky, M. D. Perry, B. M. Mammini, W. Small, and B. C. Stuart, "Plasma mediated ablation of biological tissues with nanosecond-to-femtosecond laser pulses: Relative role of linear and nonlinear absorption," *Ieee Journal of Selected Topics in Quantum Electronics*, vol. 2, pp. 801-809, 1996/12// 1996.

[58] G. Olivie, D. Giguere, F. Vidal, T. Ozaki, J. C. Kieffer, O. Nada, and I. Brunette, "Wavelength dependence of femtosecond laser ablation threshold of corneal stroma," *Optics Express*, vol. 16, pp. 4121-4129, 2008/03/17/ 2008.

[59] L. Hoffart, P. Lassonde, F. Légaré, F. Vidal, N. Sanner, O. Utéza, M. Sentis, J. C. Kieffer, and I. Brunette, "Surface ablation of corneal stroma with few-cycle laser pulses at 800 nm," *Optics Express*, vol. 19, pp. 230-240, 2011/01/03/ 2011.

[60] J. M. Krauss, C. A. Puliafito, and R. F. Steinert, "Laser interactions with the cornea," *Survey of Ophthalmology*, vol. 31, pp. 37-53, 1986/08//Jul- undefined 1986.

[61] R. Vinciguerra, A. Borgia, C. Tredici, and P. Vinciguerra, "Excimer laser tissue interactions in the cornea," *Experimental Eye Research*, vol. 206, p. 108537, 2021/05/01/ 2021.

[62] A. E. Siegman, *Lasers*: University Science Books, 1986.

APPENDIX A SKIN LASER DAMAGE THRESHOLD TABLES

A compilation of the documented single-pulse skin laser damage thresholds between 1400 nm and 2000 nm is provided below.

Table A.1. Skin laser damage thresholds between 1400 and 2000 nm

Wavelength (nm)	Pulse Duration	Beam Diameter (mm)	Threshold (J/cm^2)	Lower Fiducial (J/cm^2)	Upper Fiducial (J/cm^2)	Species	Reference
1540	600 µs	0.7	20	18.00	21.00	Yucatan	[6]
1540	600 µs	1.0	8.1	7.50	8.70	Yucatan	[6]
1540	600 µs	5.0	7.4	7.00	7.80	Yucatan	[6]
1540	31 ns	5.0	6.1	5.50	6.50	Yucatan	[6]
1540	800 µs	0.62	43.1	41.3	44.8	Yorkshire	[7]
1540	800 µs	0.57	53.5	50.8	56.2	Yucatan	[7]
1540	600 µs	0.7	15	-	-	Yucatan	[8]
2000	0.25 s	4.83	3.57	3.19	6.77	Yucatan	[9]
2000	0.5 s	4.83	4.07	2.76	6.82	Yucatan	[9]
2000	1 s	4.83	5.08	3.49	8.57	Yucatan	[9]
2000	2.5 s	4.83	5.59	3.96	9.55	Yucatan	[9]
2000	0.25 s	9.65	2.89	2.54	5.43	Yucatan	[9]
2000	0.5 s	9.65	3.38	3.19	6.57	Yucatan	[9]
2000	1 s	9.65	3.94	3.46	7.40	Yucatan	[9]
2000	2.5 s	9.65	4.82	4.44	9.26	Yucatan	[9]
2000	0.25 s	14.65	2.39	2.32	4.71	Yucatan	[9]
2000	0.5 s	14.65	2.51	2.27	4.78	Yucatan	[9]
2000	1 s	14.65	2.98	2.35	5.33	Yucatan	[9]
2000	2.5 s	14.65	3.65	3.20	6.85	Yucatan	[9]
1940	10 ms	4.8	1.11	0.95	1.23	Yucatan	[13]
1940	70 ms	4.8	4.51	-	-	Yucatan	[13]
1940	10 s	4.8	11.2	9.67	12.0	Yucatan	[13]
1940	50 ms	10	1.48	1.20	1.66	Yucatan	[13]
1940	70 ms	18	1.47	1.31	1.61	Yucatan	[13]
1940	10 s	18	2.25	2.11	2.39	Yucatan	[13]

The multi-pulse pulse skin laser damage thresholds at 1940 nm from DeLisi *et al*. [14, 15] are listed in the following table.

Table A.2. Multiple-pulse skin laser damage thresholds at 1940 nm with a pulse duration of 500 µs, from DeLisi *et al*. [14, 15]

Beam Diameter (mm)	Number of Pulses	Pulse Repetition Frequency (Hz)	Duty Cycle (%)	Exposure Time (s)	Threshold ED_{50} per Pulse (mJ/cm^2)	Lower Fiducial (mJ/cm^2)	Upper Fiducial (mJ/cm^2)
13	20	100	5	0.2	101.7	91.91	107.0
13	50	100	5	0.5	52.5	47.92	58.31
13	100	100	5	1	33.53	29.08	37.22
11	300	100	5	3	9.17	8.44	10.06
11	1000	100	5	10	5.03	4.62	5.40
11	3000	100	5	30	3.53	3.31	3.78
13	20	200	10	0.1	84.4	79.11	92.67
13	50	200	10	0.25	38.95	32.85	40.31
13	100	200	10	0.5	25.69	23.43	26.52
11	300	200	10	1.5	7.06	6.45	7.62
11	1000	200	10	5	3.63	3.30	3.96
11	3000	200	10	15	1.98	1.83	2.14
13	20	1000	50	0.02	75.2	70.29	79.11
13	50	1000	50	0.05	29.54	22.83	31.42
13	100	1000	50	0.1	17.78	16.42	18.83
11	300	1000	50	0.3	5.8	-	-
11	1000	1000	50	1	2.89	2.51	3.09
11	3000	1000	50	3	1.14	1.24	1.53

APPENDIX B CORNEA LASER DAMAGE THRESHOLD TABLES

The following three tables contain the corneal damage thresholds from the reviewed literature between 1318 nm and 1410 nm (Table B.1), 1540 nm and 1573 nm (Table B.2), and 1732 nm and 2840 nm (Table B.3). The relevant laser wavelength, pulse duration, beam diameter, radiant exposure threshold, species, and literature source are listed in each table. For most studies, the criteria for determining the MVL was a visible change in the appearance of the cornea as evaluated with a slit lamp biomicroscope 1 h post exposure. However, Courant *et al*. utilized histological analysis 1 h post exposure [44], McCally *et al*. used the data from the 30 min post exposure slit lamp examination to determine the ED_{50} [40, 41], while references [38, 39, 43, 48] used the 24 h post exposure evaluations. References [33, 37, 50] used a visible change in the appearance of the cornea as evaluated with a slit lamp biomicroscope to determine the ED_{50} but do not specify the time after exposures used in the evaluation.

Table B.1. Corneal damage thresholds between 1318 nm and 1410 nm

Wavelength (nm)	Pulse duration	Beam diameter (mm)	Threshold ED_{50} per Pulse (J/cm^2)	Uncertainty or Lower Fiducial (J/cm^2)	Upper Fiducial (J/cm^2)	Sample	Reference
1318	0.2 – 1 s	1	175	--	--	In vivo DB rabbits	[49]
1318	0.2 – 1 s	1	72	--	--	In vivo rhesus	[49]
1320	150 µs	0.4	91.6	± 9	--	In vivo chinchilla blue rabbits	[50]
1338	5 ms	0.28	70.3	68.6	71.9	In vivo NZ rabbits	[53]
1338	5 ms	0.94	35.6	33.8	36.3	In vivo NZ rabbits	[53]
1338	5 ms	1.91	29.6	28.3	30.8	In vivo NZ rabbits	[53]
1338	5 ms	3.55	30.3	28.8	31.8	In vivo NZ rabbits	[53]
1356	0.2 – 1 s	0.7	58	--	--	In vivo DB rabbits	[49]
1356	0.2 – 1 s	0.7	86.9	--	--	In vivo rhesus	[49]
1410	25 ns	1.09	2.42	--	--	In vivo rabbit	[34]

Table B.2. Corneal damage thresholds, 1540 nm to 1573 nm

Wavelength (nm)	Pulse duration	Beam diameter (mm)	Threshold ED_{50} per Pulse (J/cm^2)	Uncertainty or Lower Fiducial (J/cm^2)	Upper Fiducial (J/cm^2)	Sample	Reference
1540	2 ms	2	7.2	± 0.6	--	In vivo chinchilla blue rabbits	[50]

1540	1 ms	1.5	7.2	± 0.6	--	In vivo chinchilla rabbit	[36]
1540	40 ns	1.5	4.7	± 0.6	--	In vivo chinchilla rabbit	[36]
1540	50 ns	2	No damage	--	--	In vivo owl monkeys	[35]
1540	50 ns	0.57	21	--	--	In vivo owl monkeys	[35]
1540	800 µs	0.002 cm^2	56.7	54.9	58.9	In vivo DB rabbit	[38]
1540	800 µs	0.003 cm^2	83.7	80.5	90.6	In vitro CE	[38]
1540	930 µs	2.1	No damage	--	--	In vivo rhesus	[37]
1540	930 µs	1	9.6	--	--	In vivo rhesus	[37]
1540	36 ms	1	6.62	--	--	In vivo NZ rabbits	[41]
1540	56 ms	1	8.4	--	--	In vivo NZ rabbits	[41]
1540	110 ms	1	10.4	--	--	In vivo NZ rabbits	[41]
1540	255 ms	1	14.6	--	--	In vivo NZ rabbits	[41]
1540	1.04 s	0.5	70.1	--	--	In vivo NZ rabbits	[40]
1540	1.04 s	1	32.3	--	--	In vivo NZ rabbits	[40]
1540	1.04 s	2	14.7	--	--	In vivo NZ rabbits	[40]
1540	1.04 s	5	12.8	--	--	In vivo NZ rabbits	[40]
1540	2.05 s	0.5	116	--	--	In vivo NZ rabbits	[40]
1540	2.05 s	1	59.4	--	--	In vivo NZ rabbits	[40]
1540	2.05 s	2	28.9	--	--	In vivo NZ rabbits	[40]
1540	2.05 s	7	18.9	--	--	In vivo NZ rabbits	[40]
1540	11 s	0.5	367	--	--	In vivo NZ rabbits	[40]
1540	11 s	1	158	--	--	In vivo NZ rabbits	[40]
1540	11 s	2	79.3	--	--	In vivo NZ rabbits	[40]
1540	11 s	7	40.3	--	--	In vivo NZ rabbits	[40]
1540	100 s	2	370	--	--	In vivo NZ rabbits	[40]
1540	100 s	7	137	--	--	In vivo NZ rabbits	[40]

1550	1 s	1.85	No damage	--	--	In vivo DB rabbit	[43]
1550	10 s	1.85	No damage	--	--	In vivo DB rabbit	[43]
1550	100 s	1.85	4.6	--	--	In vivo DB rabbit	[43]
1573	3 ns	0.4	26.6	23.5	30.4	In vivo Fauve De Bourgogne	[44]

Table B.3. Corneal damage thresholds between 1732 nm and 2840 nm

Wavelength (nm)	Pulse duration	Beam diameter (mm)	Threshold ED_{50} per Pulse (J/cm^2)	Uncertainty or Lower Fiducial (J/cm^2)	Upper Fiducial (J/cm^2)	Sample	Reference
1732	225 µs	0.515	29	27	31	In vivo rhesus	[45]
1732	225 µs	0.74	26	23	29	In vivo rhesus	[45]
1732	225 µs	0.92	22	20	23	In vivo rhesus	[45]
1960	2 ms	2	2.9	± 0.5	--	In vivo chinchilla blue rabbits	[50]
2000	100 ms	1.17	23.6	± 0.3	--	In vivo DB rabbit	[46]
2000	300 ms	1.17	38.5	± 0.9	--	In vivo DB rabbit	[46]
2000	500 ms	1.17	58.2	± 0.6	--	In vivo DB rabbit	[46]
2000	1.0 s	1.17	114.9	± 5.1	--	In vivo DB rabbit	[46]
2000	2.0 s	1.17	175.2	± 3.8	--	In vivo DB rabbit	[46]
2000	4.0 s	1.17	292.8	± 3.2	--	In vivo DB rabbit	[46]
2000	100 ms	4.02	227.28	± 4.5	--	In vivo DB rabbit	[46]
2000	300 ms	4.02	302.2	± 5.8	--	In vivo DB rabbit	[46]
2000	500 ms	4.02	394.0	± 2.8	--	In vivo DB rabbit	[46]
2000	1.0 s	4.02	538.2	± 60.8	--	In vivo DB rabbit	[46]
2000	2.0 s	4.02	804.8	± 97	--	In vivo DB rabbit	[46]
2000	4.0 s	4.02	1214.4	± 14.0	--	In vivo DB rabbit	[46]
2090	2 ms	0.4	9.3	± 1.1	--	In vivo chinchilla blue rabbits	[52]
2840	2 ms	2	0.19	± 0.03	--	In vivo chinchilla blue rabbits	[50]

Table B.4 lists the threshold for cataract formation where the asterisk refers to the formation of an indirect cataract.

Table B.4. Direct and indirect cataract formation threshold

Wavelength (nm)	Pulse duration	Beam diameter (mm)	Threshold (J/cm^2)	Sample	Reference
1318	0.2 – 1 s	1	260	In vivo DB rabbits and rhesus	[49]
1318	0.2 – 1 s	1	130*	In vivo DB rabbits and rhesus	[49]
1356	0.2 – 1 s	0.7	116	In vivo DB rabbits	[49]
1356	0.2 – 1 s	0.7	434.5	In vivo rhesus	[49]

* Indirect cataract

APPENDIX C CORNEA LASER ABLATION THRESHOLD TABLES

The following tables contain the corneal ablation radiant exposure thresholds for the reviewed literature, and includes laser wavelength, pulse duration, beam diameter, sample type, and source for each threshold.

Table C.1. Corneal ablation thresholds at 800 nm

Wavelength (nm)	Pulse duration	Beam diameter (mm)	Threshold ED_{50} per Pulse (J/cm^2)	Uncertainty or Lower Fiducial (J/cm^2)	Upper Fiducial (J/cm^2)	Sample	Reference
800	100 fs	0.008	1.24	1.06	1.43	Epithelium. Excised porcine eyes.	[54]
800	300 fs	0.008	1.41	1.20	1.63	Epithelium. Excised porcine eyes.	[54]
800	500 fs	0.008	1.57	1.33	1.81	Epithelium. Excised porcine eyes.	[54]
800	800 fs	0.008	1.68	1.42	1.90	Epithelium. Excised porcine eyes.	[54]
800	1 ps	0.008	1.94	1.65	2.33	Epithelium. Excised porcine eyes.	[54]
800	2 ps	0.008	2.38	2.04	2.76	Epithelium. Excised porcine eyes.	[54]
800	3 ps	0.008	2.98	2.55	3.46	Epithelium. Excised porcine eyes.	[54]
800	5 ps	0.008	3.52	3.01	4.06	Epithelium. Excised porcine eyes.	[54]
800	100 fs	0.008	1.51	1.27	1.73	Stroma. Excised porcine eyes.	[54]
800	300 fs	0.008	1.6	1.35	1.84	Stroma. Excised porcine eyes.	[54]
800	500 fs	0.008	1.89	1.60	2.16	Stroma. Excised	[54]

						porcine eyes.	
800	800 fs	0.008	1.96	1.67	2.26	Stroma. Excised porcine eyes.	[54]
800	1 ps	0.008	2.27	1.92	2.62	Stroma. Excised porcine eyes.	[54]
800	2 ps	0.008	2.5	2.12	2.87	Stroma. Excised porcine eyes.	[54]
800	3 ps	0.008	3.13	2.67	3.59	Stroma. Excised porcine eyes.	[54]
800	5 ps	0.008	4.77	4.06	5.52	Stroma. Excised porcine eyes.	[54]

Table C.2. Corneal ablation thresholds between 1025 nm and 1064 nm

Wavelength (nm)	Pulse duration	Beam diameter (mm)	Threshold ED_{50} per Pulse (J/cm^2)	Uncertainty or Lower Fiducial (J/cm^2)	Upper Fiducial (J/cm^2)	Sample	Reference
1025	450 fs	0.0107	2.7	± 0.1	--	Epithelium. Human corneas.	[30]
1025	450 fs	0.0107	5.6	± 0.4	--	Epithelium. Human corneas.	[30]
1025	450 fs	0.0107	3.4	± 0.1	--	Bowman's layer. Human corneas.	[30]
1025	450 fs	0.0107	7.1	± 1.1	--	Bowman's layer. Human corneas.	[30]
1053	30 ps	0.005	20	27	15	Human corneas.	[55]
1053	60 ps	0.005	26	36	20	Human corneas.	[55]
1053	200 ps	0.005	40	58	32	Human corneas.	[55]
1053	350 fs	0.5	0.28	--	--	Excised porcine eyes.	[57]

1053	20 ps	0.5	7	--	--	Excised porcine eyes.	[57]
1053	150 ps	0.5	25	--	--	Excised porcine eyes.	[57]
1053	900 ps	0.5	64	--	--	Excised porcine eyes.	[57]
1000 – 1060, 1053, 1064	20 ps	NA	4.8	--	--	Stroma. Excised porcine eyes.	[56]
1000 – 1060, 1053, 1064	2.86 ps	NA	1.69	--	--	Stroma. Excised porcine eyes.	[56]
1000 – 1060, 1053, 1064	1.6 ps	NA	1.19	--	--	Stroma. Excised porcine eyes.	[56]
1000 – 1060, 1053, 1064	800 fs	NA	0.6	--	--	Stroma. Excised porcine eyes.	[56]

NA – Not available